Nat Hazards (2012) 60:879–914
DOI 10.1007/s11069-011-9874-9

ORIGINAL PAPER

Potentials and constraints of different types of soil moisture observations for flood simulations in headwater catchments

Axel Bronstert · Benjamin Creutzfeldt · Thomas Graeff · Irena Hajnsek · Maik Heistermann · Sibylle Itzerott · Thomas Jagdhuber · David Kneis · Erika Lück · Dominik Reusser · Erwin Zehe

Received: 8 March 2010 / Accepted: 7 June 2011 / Published online: 13 August 2011

Abstract Flood generation in mountainous headwater catchments is governed by rainfall intensities, by the spatial distribution of rainfall and by the state of the catchment prior to the rainfall, e.g. by the spatial pattern of the soil moisture, groundwater conditions and possibly snow. The work presented here explores the limits and potentials of measuring soil moisture with different methods and in different scales and their potential use for flood simulation. These measurements were obtained in 2007 and 2008 within a comprehensive multi-scale experiment in the Weisseritz headwater catchment in the Ore-Mountains, Germany. The following technologies have been applied jointly thermogravimetric method, frequency

A. Bronstert (✉) · T. Graeff · M. Heistermann · D. Kneis · E. Lück
Institute for Earth and Environmental Sciences, University of Potsdam,
Karl-Liebknecht-Str. 24-25, 14476 Potsdam, Germany
e-mail: axelbron@uni-potsdam.de

B. Creutzfeldt
GFZ German Research Centre for Geoscience, Section 5.4: Hydrology, Telegrafenberg,
14473 Potsdam, Germany

I. Hajnsek
ETH Zurich, Institute of Environmental Engineering, Schafmattstr. 6,
8093 Zurich, Switzerland & German Aerospace Center, Microwaves
and Radar Institute, P.O. Box 1116, 82234 Wessling, Germany

S. Itzerott
GFZ German Research Centre for Geoscience, 1.4: Remote Sensing, Telegrafenberg,
14473 Potsdam, Germany

T. Jagdhuber
German Aerospace Centre, Microwaves and Radar Institute, P.O. Box 1116,
82234 Wessling, Germany

D. Reusser
Potsdam Institute for Climate Impact Research, P.O. Box 601203, 14412 Potsdam, Germany

E. Zehe
Karlsruhe Institute of Technology KIT, Institute of Water Resources and River Basin Management,
Kaiserstrasse 12, 76129 Karlsruhe, Germany

domain reflectometry (FDR) sensors, spatial time domain reflectometry (STDR) cluster, ground-penetrating radar (GPR), airborne polarimetric synthetic aperture radar (polarimetric SAR) and advanced synthetic aperture radar (ASAR) based on the satellite Envisat. We present exemplary soil measurement results, with spatial scales ranging from point scale, via hillslope and field scale, to the catchment scale. Only the spatial TDR cluster was able to record continuous data. The other methods are limited to the date of over-flights (airplane and satellite) or measurement campaigns on the ground. For possible use in flood simulation, the observation of soil moisture at multiple scales has to be combined with suitable hydrological modelling, using the hydrological model WaSiM-ETH. Therefore, several simulation experiments have been conducted in order to test both the usability of the recorded soil moisture data and the suitability of a distributed hydrological model to make use of this information. The measurement results show that airborne-based and satellite-based systems in particular provide information on the near-surface spatial distribution. However, there are still a variety of limitations, such as the need for parallel ground measurements (Envisat ASAR), uncertainties in polarimetric decomposition techniques (polarimetric SAR), very limited information from remote sensing methods about vegetated surfaces and the non-availability of continuous measurements. The model experiments showed the importance of soil moisture as an initial condition for physically based flood modelling. However, the observed moisture data reflect the surface or near-surface soil moisture only. Hence, only saturated overland flow might be related to these data. Other flood generation processes influenced by catchment wetness in the subsurface such as subsurface storm flow or quick groundwater drainage cannot be assessed by these data. One has to acknowledge that, in spite of innovative measuring techniques on all spatial scales, soil moisture data for entire vegetated catchments are still today not operationally available. Therefore, observations of soil moisture should primarily be used to improve the quality of continuous, distributed hydrological catchment models that simulate the spatial distribution of moisture internally. Thus, when and where soil moisture data are available, they should be compared with their simulated equivalents in order to improve the parameter estimates and possibly the structure of the hydrological model.

Keywords Soil moisture · Remote sensing · Hydrological modelling · Flood forecasting · Soil moisture measurement comparison

1 Introduction

1.1 Flood generation in headwater catchments and the role of soil moisture

Flood generation in mountainous headwater catchments is governed by conditions that make flood simulations particularly challenging. The outflow from these catchments is generally large and responds quickly to storm events: slopes are typically steep, the storage capacity of shallow soils is low and, due to high average precipitation and low average temperatures, the initial soil moisture is often increased compared with other environments. In addition, headwater catchments are typically small. Therefore, the flood simulation is not only sensitive to errors in the observed and predicted rainfall intensities but it is particularly sensitive to errors in the observed and predicted spatial distribution of rainfall. In consequence, reliable flood warnings can be issued only for short lead times. Short lead times, together with short response times, constitute the particular threat posed by floods in such flashy catchments.

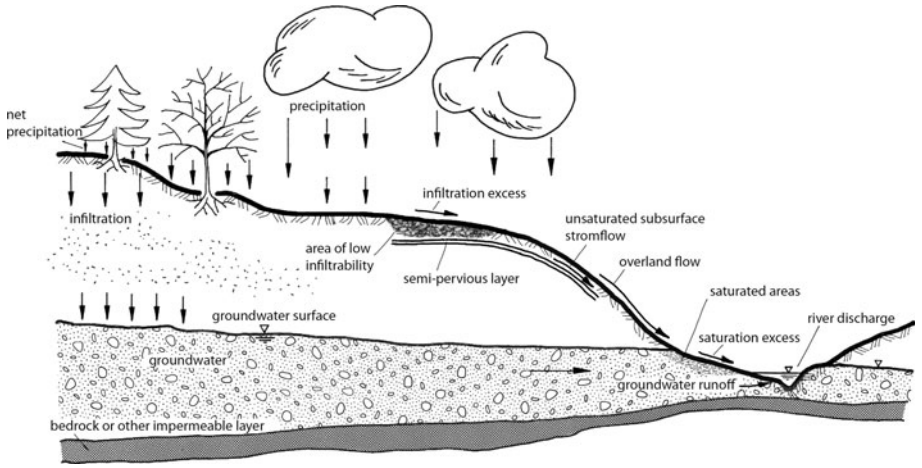

Fig. 1 Scheme of flood runoff generation processes (from Bronstert 2005)

The magnitude of a mountain flood is governed by the spatial–temporal pattern of the rainstorm (Bronstert and Bárdossy 2003; Ehret 2003; Zehe et al. 2005) and, due to the nonlinear behaviour of the runoff generation processes (Uhlenbrook and Leibundgut 2002), by the state of the catchment prior to the rainfall, e.g. by the spatial pattern of the soil moisture and the groundwater conditions (most relevant is the depth of the water table below the ground surface). The subsurface water conditions (both soil moisture and groundwater) control the landscape capacity to store rainfall water (Merz and Plate 1997; Zehe and Blöschl 2004; Bronstert and Bárdossy 1999; Grayson and Blöschl 2001).

Flood runoff comprises different runoff generation processes, such as overland flow caused either by infiltration excess ('Hortonian runoff') or by saturation excess ('saturation runoff'), subsurface storm flow (e.g. quick lateral flow due to transient saturation conditions close to the soil surface or in a coarse soil layer overlying a zone of little or no permeability, such as plough layer, argillic horizon or bedrock), or by a relatively quick groundwater drainage into the channel system triggered by a steeper gradient of the groundwater surface after heavy rainfall. Figure 1 depicts these flood runoff generation processes on a hillslope scale.

The magnitude of most runoff generation processes depends on the wetness in the particular catchment through the following mechanisms (see Fig. 2):

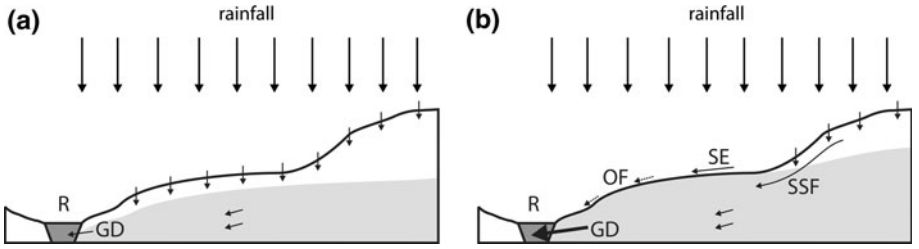

Fig. 2 Different runoff generation mechanisms for low and high catchment wetness (adapted from Dunne et al. 1975): **a** before or at the start of the rainfall event: mainly groundwater drainage (GD) into the river R; **b** after long rainfall period: increase in groundwater level, partially up to the land-surface generating saturation excess SE and partially subsurface stormflow SSF towards R

- High catchment wetness is expressed by a relatively high groundwater table and steeper gradients of the groundwater surface. Additional rainfall will further enhance *groundwater exfiltration* into the channel system.
- A high groundwater table also induces the unsaturated soil zone (between the soil surface and the groundwater) to become rather shallow or even allow the groundwater level to reach the soil surface. Rainfall on such areas can hardly infiltrate and will cause *saturation overland flow* from the saturated areas into the channel.
- High soil moisture values boost the occurrence of *subsurface storm flow* mechanisms, such as the quick subsurface transfer of infiltration water downslope towards the channel system (Weiler and McDonnell 2007), thus contributing to overall flood runoff.

One should keep in mind that some other runoff generating processes, such as infiltration excess due to silted, crusted or even impermeable surfaces, do not depend primarily on catchment wetness. Nonetheless, it has long been recognised (Dunne et al. 1975) that in the case of subsurface-dominated flood generation mechanisms, a profound knowledge of the catchment wetness conditions (average values, and possibly also the areal and vertical distribution) prior to a rainstorm is considered to be an important information for an improved forecast performance for flood runoff.

1.2 Key issues of flood simulations in headwater catchments: storm precipitation and pre-event soil moisture

The simulation of flood events can have different intentions, e.g. for analysing the hydrological process mechanisms and their interactions in generating floods, the assessment and comparison of potential flood reduction measures or the forecasting of a flood discharge in the river. Figure 3 shows the components of a typical forecasting system for floods in a headwater catchment. Starting from an initialisation of the system state variables, a rainfall-runoff model is driven by meteorological observations. Based on the observed rainfall intensities only, the lead time is limited to the system's response time. To enhance the lead time, meteorological forecasts are used as boundary conditions in the forecast period.

Hydrological forecasts could be substantially improved by enhancing the spatial precision of rainfall observation and forecasts (Collier 2007; Younis et al. 2008). In particular, a superior observation and regionalisation of rainfall will improve the representation of the system's state variables and thus reduce the uncertainty of a hydrological forecast. However, the estimated meteorological input will always be subject to error. As a result,

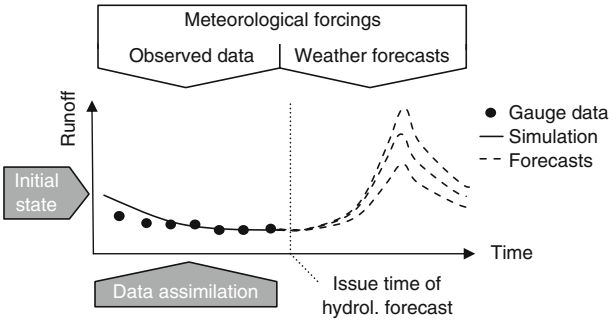

Fig. 3 Components of a flood forecasting system for small mountainous catchments based on rainfall-runoff modelling

the state variables will never be perfectly represented. This holds true particularly for state variables, which are related to subsurface water storage and are thus considered to have an essential impact on runoff generation (Aubert et al. 2003). The catchment conditions reflected by these state variables are typically referred to as *pre-event soil moisture* or *antecedent wetness*. A variety of strategies are available in order to cope with the issue of pre-event moisture. Traditional approaches for event-based models consider the previous rainfall (antecedent precipitation index, API) or the current catchment outflow as an indicator of subsurface storage (Fedora and Beschta 1989; Pilgrim and Cordery 1993; Berthet et al. 2009, Marchi et al. 2010). For continuous rainfall-runoff models, state variables or model parameters are usually updated by assimilating the observed stream flow prior to issuing a hydrological forecast (Refsgaard 1997).

Even though the relevance of catchment wetness for flash flood generation has been analysed recently (e.g. by Borga et al. 2007), real soil moisture data are hardly used for flash flood prediction. In contrast, (Marchi et al. 2010) have used antecedent precipitation as significant descriptor of runoff coefficients for flash flood events in their analysis of many European catchments, including the Weisseritz. Nevertheless, the past 10 years have witnessed a development towards the direct integration of observed soil moisture. This comprises the use of ground-based point measurements (e.g. by TDR probes) as well as remotely sensed soil moisture patterns (e.g. by the ERS scatterometer) or combinations of both. Soil moisture patterns have been used to initialise state variables (Goodrich et al. 1994; Jacobs et al. 2003; Weissling et al. 2007; Brocca et al. 2009; Noto et al. 2008) and to update state variables by assimilation techniques (Pauwels et al. 2002; Aubert et al. 2003; Francois et al. 2003; Crow et al. 2005). In addition, Parajka et al. (2006) explored the potential to use remotely sensed soil moisture for model calibration and validation. Most authors report that the use of soil moisture data increased the quality of hydrological forecasts. However, according to Crow and Ryu (2009), the improvements achieved through these efforts have been comparably low. They argue that antecedent moisture conditions are of minor importance for intense storm events and that the error from the estimation of antecedent soil moisture might be low compared with the error introduced by rainfall estimation. Beyond this, they criticise the fact that assimilation techniques designed for linear models might be ill-suited for the nonlinear relationship between antecedent soil moisture and runoff. In general, the highest benefit from the assimilation of remotely sensed soil moisture can be expected for ungauged basins where the assimilation of stream flow data is not an option (Lakshmi 2004).

Despite (or because of) the above criticism, further research is required to explore the limits and potentials of soil moisture assimilation in rainfall-runoff models. In this context, an important question is, '*How can soil moisture observations be related to the model's state variables*?' The answer to this question is—on the one hand—subject to the modelling concept (e.g. lumped vs. distributed, event-based vs. continuous). For example, it has been shown that the nonlinearity of the rainfall-runoff observation could better be captured if spatially distributed soil moisture data were preferred over spatial averages (Bronstert and Bárdossy 1999; Merz and Bárdossy 1998; Noto et al. 2008). On the other hand, the answer to the above question is subject to the spatio-temporal scale of observation (Western et al. 2002). Observations might be characterised, e.g. by point- versus volume-integrated technologies, spatial resolution or point density, vertical range and vertical resolution as well as temporal resolution. In order to develop optimal assimilation strategies, we have to improve our understanding of scale transitions in the observation of soil moisture. For this purpose, the observation of soil moisture at multiple scales has to be combined with modelling concepts at multiple scales. In this paper, we report on our work towards a better assessment

of pre-event soil moisture as a major regulator for the transfer of storm rainfall to flood runoff, thus focusing on the moisture assimilation component of the forecast chain.

2 Soil moisture measurements: different methods and associated scales

2.1 Variability of soil moisture at different spatial scales

Surface soil moisture varies in space and time. This variability is caused by boundary fluxes of energy and mass, such as the processes of infiltration, evaporation, plant water uptake, deep drainage, groundwater fluctuation or surface runoff. But media properties, such as soil hydraulic properties or macropores, also control the soil moisture distribution over the different domains and give feed back to the boundary conditions, whereby these properties themselves depend on the soil water content. Thus, it is a complex interplay of soil moisture and the controlling factors, implying that at different scales different processes and properties are important in this complex interaction. Blöschl and Sivapalan (1995) have worked out a concept of spatial heterogeneity of different media at different scales in a catchment. Characteristic variations in soil moisture relevant for the generation of runoff during and after heavy rainfall events can be observed in a number of different spatial scales that were affected by the properties in those scales.

At the point scale (extent: few centimetres), one can often observe differences in soil moisture over short distances, which can look like an almost random distribution. We will therefore refer to the spatial distribution at this scale as the 'micro-scale random variability'. This random variability can also be invoked by the soil moisture measurement method itself (e.g. Evett et al. 2009).

At the field scale (extent: 10–100 m) with relatively homogenous landscape features such as land use, soil types or topography, soil moisture variability is mainly controlled by soil water retention and the hydraulic conductivity, which depends primarily on the soil texture, macropores, porosity, bulk density or organic matter. At this scale, soil moisture can be considered to be rather homogenous at saturation (Harter and Zhang 1999), e.g. after a heavy rainfall event, because the spatial variability of porosity is relatively small (Corwin et al. 2006). After Vereecken et al. (2007), the soil moisture variability increases during the process of drying, until the variability reaches a maximum and by further drying decreases again. For example, Zehe and Blöschl (2004) found that the variability in soil water content observed within a cluster of 25 TDR measurements at a 4-m^2 plot was as large as the soil moisture variance observed at 61 locations in the 3.2 km^2 Northern part of the Weiherbach catchment.

At the hillslope scale (extent: 20–1,000 m), the soil moisture distribution is frequently correlated with topography (e.g. Taumer et al. 2006; Weihermuller et al. 2007), which may be directly linked to the lateral redistribution of water along the topography, but also indirectly due to differences in soil characteristics (e.g. more alluvial soils and shallow groundwater depths at the hillslope bottoms), differences in meteorological forcing (e.g. exposition to solar radiation; shadowing effects) or due to changes in land use. At this scale, the overall soil moisture pattern can be explained as organised variability type, while the possible small-scale variations can be explained as subscale random variability type.

At the catchment scale (extent: 1–100 km), especially in mountainous areas, one major source of soil moisture variability is precipitation, such as fractional and orographic rainfall or snowfall and snow melt. Ryu and Famiglietti (2005) showed that even in areas with no distinct topography, the soil moisture variability due to fractional rainfall may be

larger than soil heterogeneity. Nonetheless, different morphological landscape units (e.g. mountain slopes vs. valley bottoms or flood plains) and associated features like topography, geology, geomorphology, soil types, groundwater and interactions with surface waters (rivers and lakes) are of high relevance for soil moisture variability (Choi et al. 2007). One has to remember that groundwater is the major factor controlling soil moisture in deeper soil layers and thus partly controlling runoff generation processes.

2.2 Set-up of the multi-scale soil moisture observation experiment

Various studies (Wagner et al. 2004; Robinson et al. 2008a, b; Vereecken et al. 2008) have discussed different sensor techniques to monitor soil moisture at several hydrologically important scales. Techniques covering larger scales (mainly by remote sensing) have generally a low penetration depth (a few centimetres), which is why the information obtained for deeper soils are limited (Martinez et al. 2008). In addition, they have a relatively coarse resolution in space and time, so they do not capture small-scale variability, and remote sensing-based estimation of soil moisture beneath a vegetation cover is disturbed depending on the density of the coverage (see, e.g. Sects. 3.2 and 3.3 in this paper). On the other hand, small-scale, ground-based measurements have the ability to measure small-scale variability and soil moisture at different depths of interest, but the sampling size and the total spatial coverage are very limited. However, no measurement technology exists capable of measuring soil moisture in any desired spatial resolution and temporal frequency. Thus, the aim of this study is to integrate the positive properties of the different measurement technologies and sensors and to assess the potentials of such observations for a subsequent use in flood simulations.

We selected the Weisseritz catchment in the Ore-Mountains, Saxony, Germany, as the investigation area, which is known for severe flood events, i.e. very fast and intense runoff response after heavy precipitation events. The Weisseritz basin is located between 50°40′ and 51°03′ northern latitude and 13°31′ and 13°45′ eastern longitude (see Fig. 4).

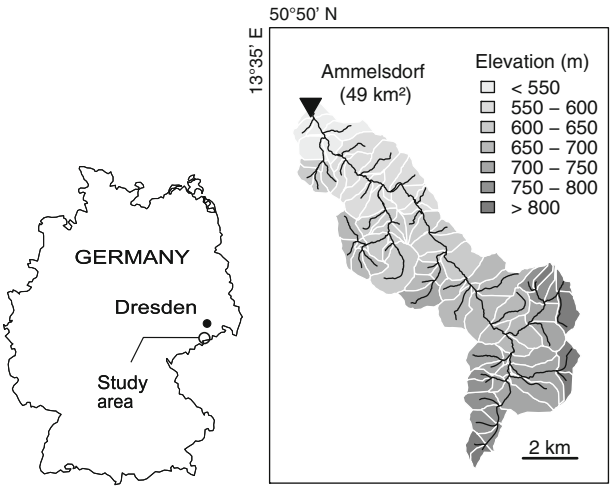

Fig. 4 Location of the Weisseritz catchment (*left*), and the headwater upstream gauge Ammelsdorf (*right*). The *triangle* indicates the location of the stream gauge. The *white lines* display subcatchment boundaries (not used in this study)

It contains two main channels, the Red and the Wild Weisseritz, which jointly contribute to the Elbe River in the city of Dresden. The whole basin covers an area of 384 km^2 and stretches over 15 km from north to south, with an average elevation of approximately 730 m asl (ranging between 910 m asl and 120 m asl at the inflow into the Elbe River in Dresden). About 60% of the basin is forest, dominated by conifers, while 20% grasslands, 10% arable land, 4% upland bog, and 6% settlements characterise the remaining parts of the catchment. Annual rainfall is approximately 950–1,050 mm, and average annual temperature is between 4 and 5.5°C. The headwater catchment upstream of the gauge at Ammelsdorf (catchment area: 49.3 km^2, altitude ranging between 910 m asl and 527 m asl, see Fig. 4) is the experimental area where the multi-scale soil moisture measurements have been taken and various flood events have been simulated.

At the point scale, near-surface soil moisture was measured on selected days (field campaign snapshots, conducted by approx. five persons simultaneously) with fairly high areal resolution by using hand-held Theta probes. In addition, for calibration purposes, thermogravimetric moisture measurements of soil samples have been executed. At the field scale, spatial time domain reflectometry (STDR) clusters have been installed at two locations within the headwater to record the small-scale variability (in area and depth) and the temporal dynamics of the soil moisture at those areas over a period of several years. On the same days as the field campaigns, ground-penetrating radar (GPR) observations were made at the field and hillslope scales (two sites). At the catchment scale, a campaign for airborne multi-polarisation microwave remote sensing was conducted, and for the whole catchment, active microwave satellite remote sensing data were analysed to derive the near-surface soil moisture pattern.

The combination of these techniques aims to derive a multi-scale picture of the spatial distribution of the soil moisture. The remote sensing techniques were compared with ground-based observations by means of the field campaigns with the FDR (frequency domain reflectometry) probes for two intensive measurement fields (size: 50 m $\times$ 50 m; 5–10 m measurement resolution; land use: pasture and bare soil), for eight extensive measurement fields (area size: 320 m $\times$ 80 m; 20 m resolution; land uses: winter wheat, winter triticale, winter barley, winter rye, winter rape, oats, maize and grassland; measurement resolution 20 m $\times$ 20 m), and by GPR explorations on the same two fields where the intensive FDR measurements had been executed. Moreover, the continuous STDR measurements were analysed in order to identify a relationship between the near-surface (a few cm) moisture (measured during the field campaigns) and the soil layers to a depth of 60 cm. Thus, information on the soil water at some deeper soil depths was derived from the STDR results with two differing land covers and topography. Apart from the very recent work of Koyama et al. (2010), there is hardly any other study known which combines so many different sensor methods and measurement scales. The properties of the applied technologies are listed in Table 1, and Fig. 5 depicts an overview of the different spatial scales related to these technologies.

Besides the thermogravimetric measurements, all applied techniques are based on the reflection of electromagnetic waves and the estimation of the electrical permittivity. There is a petro-physical relationship between electrical permittivity and soil moisture, which depends on soil texture, clay content, organic content and bulk density. A broad overview of different petro-physical models is given by Lesmes and Friedman (2005). Here, we used a linear relationship proposed by Herkelrath et al. (1991), which has been adapted to the specific site conditions. This relationship formed the basis for all subsequent transformations of the measured signals of FDR (Theta probe), GPR and STDR sensors. In the following, we briefly summarise the different scale-specific measurement techniques applied in this study.

Table 1 Properties of the different measurement types used to observe soil moisture at different scales

Name	Physical principle	Sampling volume (m^3)	Spatial extent	Resolution in space	Frequency (resolution in time)	Comments	References
Thermo-gravimetric	Weighting of wet and dry soil samples (destructive)	~0.0001	Optional	Optional	Destructive; not repeatable	Conventional method	
FDR (Theta probe)	Permittivity by the relative impedance (invasive)	~0.0001	Optional (area); 6 cm (depth)	Horiz: (optional) Vert: integral value	(Sampling campaign dependent)	Hand-held version; easy and cheap measurement	Gaskin and Miller (1996)
Spatial TDR cluster	Permittivity by electromagnetic wave velocity (invasive)	~0.0001	~25 × 25 m (area); 60 cm (depth)	Horiz: ~1–5 m Vert: ~10 cm	Continuous	Non-standard device	Robinson et al. (2003) and Graeff et al. (2010)
Ground-penetrating radar (GPR)	Permittivity by electromagnetic wave velocity (non-invasive)	~0.01	~100 × 100 m (area); ~5–20 cm (depth)	Horiz: (optional) Vert: integral value	(Sampling campaign dependent)	Applies only for the direct groundwave technique; device expensive	Huismann et al. (2003)
Polarimetric SAR	Polarimetric decomposition techniques based on electromagnetic models (non-invasive)	~0.2	~10–100 km^2 (area); ~5–20 cm (depth, depending on wave length), e.g. ~2–12 cm (depth at L-Band)	Horiz: 2 × 1 m (L-band) Vert: integral value	(Aircraft flight dependent)	Strong influence of vegetation; costly	Hajnsek et al. (2009)
Envisat ASAR	Backscattering coefficient analysis (non-invasive)	~50	100–1,0000 km^2 (area); ~5 cm (depth)	Horiz: 25 × 25 m Vert: integral value	Several times per month (unsteady)	Strong influence of vegetation; ground measurements required	Baghdadi et al. (2006)

2.2.1 Plot scale

Thermogravimetric measurements. A popular and long-existing method for measuring the soil water content is the determination of weight losses due to soil drying. The disadvantage is that it is a destructive method, so that a continuous monitoring of soil moisture is not possible. During our second measurement campaign, we collected 187 oven-dried and weighted (wet vs. dry) soil core samples (diameter = 5.6 cm, height = 4.1, volume 100 cm^3) at five different plots.

FDR probes. Hand-held FDR probes (length: 6 cm) of the type Theta probe (DELTA-T) (Gaskin and Miller 1996) were used to observe near-surface soil moisture in four measurement campaigns in April and May 2008. Two spatial sampling schemes were implemented, for both intensive and extensive sampling (see Fig. 5). For the intensively equipped scheme (two plots covered by pasture and ploughed bare soil), a spatial extent of 50 m × 50 m with a sampling resolution of 10 m × 10 m was chosen, yielding in total 57 measurement points. In the centre of the two areas, the sampling resolution was increased to 5 m × 5 m. Each point measurement was repeated three times to reduce measurement errors. The extensive schemes (eight fields covered with different types of crops) consist of areas of 320 m × 80 m with a sampling resolution of 20 m × 20 m, yielding in total 85 measurement points. Thus, the small but densely sampled area can be referred to the plot scale, while the 'extensive schemes' can be referred to the field scale (next section).

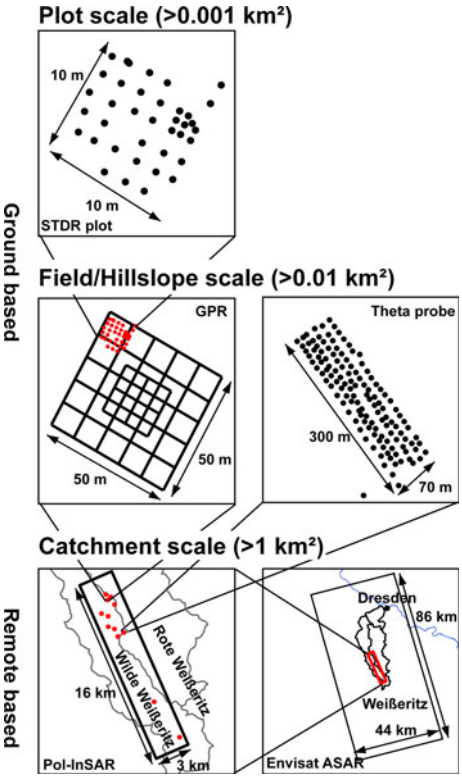

Fig. 5 Spatial arrangement of the different soil moisture measurements from the point scale (singe FDR or TDR probe), plot scale (STDR cluster), field and hillslope scale (both GPR and spatially dense, manual FDR campaigns), to the catchments scale (airborne or satellite remote sensing), conducted in Weisseritz catchment, Ore-Mountains, Saxony, Germany. Note that the measurements at the different scales are organised in a nested manner. Further explanation of measurement techniques and resolutions are given in Table 1

2.2.2 Field scale

STDR. Conventional TDR measurements (reviews are given by e.g. Robinson et al. 2003; Cassiani et al. 2006) can be used to estimate the mean soil moisture of the surrounding soil via the reflected travel time of an electromagnetic wave along the waveguide. Several authors have shown (Feng et al. 1999; Oswald et al. 2003; Schlaeger 2005; Greco 2006) that the reflected signal can deliver information on the water content along the sampled profile. To quantify the spatial distribution of the water content along the wave guide, an inverse signal analysing technology has been introduced by Graeff et al. (2010) and called it 'STDR' (spatial time domain reflectometry). The joint analysis of a number of wave guides distributed over an area of a few hundreds of m^2 (in our case 225 m^2) may yield a spatial (in area and depth) and temporal distribution of the soil moisture. We term the combination of several STDR probes as 'STDR cluster'. Our STDR clusters combine up to 39 single spatial TDR sensors of 60 cm depth. The total sampling time for all 39 sensors is about 10 min. Two STDR clusters have been installed in the headwater of the Weisseritz catchment close to the gauge Rehefeld on a hillslope covered with pasture ('pasture cluster') and on another dominated by conifer forest ('forest cluster').

GPR. GPR (ground-penetrating radar) enables the estimation of soil water content and its variation from a point up to the field scale (e.g. Galagedara et al. 2005a; Grote et al. 2002; Huisman et al. 2001, 2002; Schmalholz 2007; Van Overmeeren et al. 1997, Huisman et al. (2003). The physical principle of GPR is the same as of TDR measurement. The main difference is that TDR uses a guided electromagnetic wave, whereas the GPR technique is based on an unguided wave. In this study, we used the signal of the direct groundwave (Wollny 1999), which is the electromagnetic wave, which directly propagates below the soil surface from the transmitter to the receiver. Compared with the STDR method, the direct groundwave method enables the non-invasive and rapid collection of data over a larger area. However, it is not possible to resolve the soil moisture variation over depth. In this study, we have used an experimental GPR set-up, which has been proposed and described in detail by Huisman et al. (2001). Under these conditions, the sampling depth is 8–12 cm depending mainly on the soil moisture content (Galagedara et al. 2005b).

2.2.3 Catchment scale: SAR remote sensing

Remote sensing techniques clearly enhance the spatial coverage of surface or near-surface earth properties. Radar remote sensing can add spatial information on snow cover and soil moisture by estimating the dielectric properties and the geometric structure of bare soil surfaces through analysing the sensitivity of microwave scattering. However, these variables cannot be measured directly, and the accuracy achievable is clearly below the accuracy through ground measurements. The advantage of radar remote sensing (compared with optical remote sensing) is its cloud-independent imaging capability and its potential to acquire subsurface information dependent on the microwave frequency. Several methods have been developed to assess the soil moisture conditions on bare surfaces. However, ground surfaces in most climate zones are at least partly covered with vegetation, which makes the consideration of soil cover mandatory for such regions, in spite of the associated difficulties.

Microwave remote sensing from aircraft. A new polarimetric decomposition and inversion algorithm of the microwave signals recorded by the airborne sensors has been developed for bare fields as well as for vegetation-covered fields. For the airborne sensed vegetation cover, the ground components can be used after removal of the volume component. A range of different frequencies (X-band (9.6 GHz), C-band (5.3 GHz), L-band

(1.3 GHz), P-band (0.35 GHz)) was investigated for soil moisture estimation suitability. Finally, the L-band was identified as the most suitable for penetration into a volume of agricultural vegetation. The algorithm is not based on empirical relations and therefore does not need calibration through ground measurements. Recent publications on polarimetric decomposition techniques show their capabilities (e.g. Cloude and Pottier 1996; Freeman and Durden 1998; Yamaguchi et al. 2005; van Zyl et al. 2008; Lee and Pottier 2009), whereas the details of the polarimetric decomposition and inversion algorithm for soil moisture estimation on bare soils, as well as under vegetation, are presented by Hajnsek et al. (2009), Jagdhuber et al. (2009), Cloude and Pottier (1997) and Hajnsek et al. (2003).

Microwave remote sensing from satellites. As mentioned above, a satellite system for the estimation of soil moisture should ideally record full polarimetric data in L- or C-band, in order to ensure on the one hand the penetration depth and on the other to detect the influence of the vegetation canopy. These requirements are presently best met by the ALOS PALSAR system (L-band, full polarisation), but its data access for users is difficult. The suitability of the Envisat ASAR system, characterised by dual-polarised C-band data, is reduced concerning the moisture estimation but it is advantageous regarding data availability. Thus, for this study, data from four dates in 2008 (24th April; 3rd May; 10th May; 16th May) could be used from this system. The data were recorded in the Image (IM) mode (operation direction: Ascending/Descending), VV and VH polarisation and incident angles of 19–35 degrees. This C-band data possess a pixel size of 25 m and a penetration depth of few centimetres. Compared with the airborne system described before, the potential of the ASAR satellite-based C-band data is much reduced due to the shorter wavelength and the absence of full polarisation. Thus, substantial efforts are required to derive a ground measurement–based empirical relationship between satellite data and actual soil moisture. Therefore, in the period from 24th April to 16th May 2008, four ground measurement campaigns of the surface soil moisture were conducted on the days of the satellite overflights, monitoring eight fields of 320 m $\times$ 80 m size in a spatial resolution of 20 m by means of the Theta probe. The eight fields differ in the covering crop type, representing winter wheat, winter triticale, winter barley, winter rye, winter rape, oats, maize and grassland. In addition to soil moisture, plant development parameters (biomass, plant moisture, plant height, and proportion of coverage) were collected.

An empirical linear relationship between satellite and ground data was derived for each date guided by using the two backscattering coefficients from the satellite (in vertical polarisation and in horizontal polarisation, respectively), and the ground-measured data by FDR, both restricted to data from bare soil plots. This derivation used two-thirds of the bare plot data as training data and one-third for the validation. For every single satellite acquisition date, one specific empirical relationship was estimated and applied to all fields of arable land in the central area of the Weisseritz catchment.

3 Exemplary results of the multi-scale soil moisture observations in the Weisseritz area

3.1 Point scale to field scale: STDR clusters, GPR and FDR campaigns

3.1.1 Individual STDR probes

Figure 6 shows the high variability of soil moisture content recorded from the individual STDR probes of the STDR cluster ‘pasture’ at the location Rehefeld starting from a few

days before and lasting a few days after the measurement campaigns. The probes of the STDR cluster cover an area of approx. 15 m × 15 m. The missing data in 2008 are due to a power failure at the measurement station. The total range of the recorded soil moisture reflects small-scale heterogeneity within this plot. The soil moisture values range from 13 Vol% at probes with high gravel content to 44 Vol% where soil particles of smaller size dominate. Note that all probes show similar relative soil moisture dynamics, i.e. the absolute values differ (due to the small-scale heterogeneity) but the variations in time are much the same, which is reflected by the high correlation coefficients between the probes (> 0.90). Before the first measurement campaign, several smaller precipitation events occurred, causing an increase in water content (Fig. 6a, c). During the campaigning days, a certain drying of the soil can be seen. The second campaign in particular was characterised by drying of the soil due to water loss by evapotranspiration (Fig. 6b, c). The signals obtained from all STDR probes have been inverted, yielding vertically resolved soil moisture information (not shown here).

3.1.2 STDR and GPR measurements and FDR campaigns at the sites of the 2 STDR clusters

As part of the field campaigns, the soil moisture close to the areas of the two STDR clusters was additionally monitored at the two campaigning days by hand-held FDR probes ('Theta probes') and by GPR, respectively. The resulting data obtained by FDR and GPR are summarised in the upper graphs of Fig. 7. The data collected with the two STDR clusters

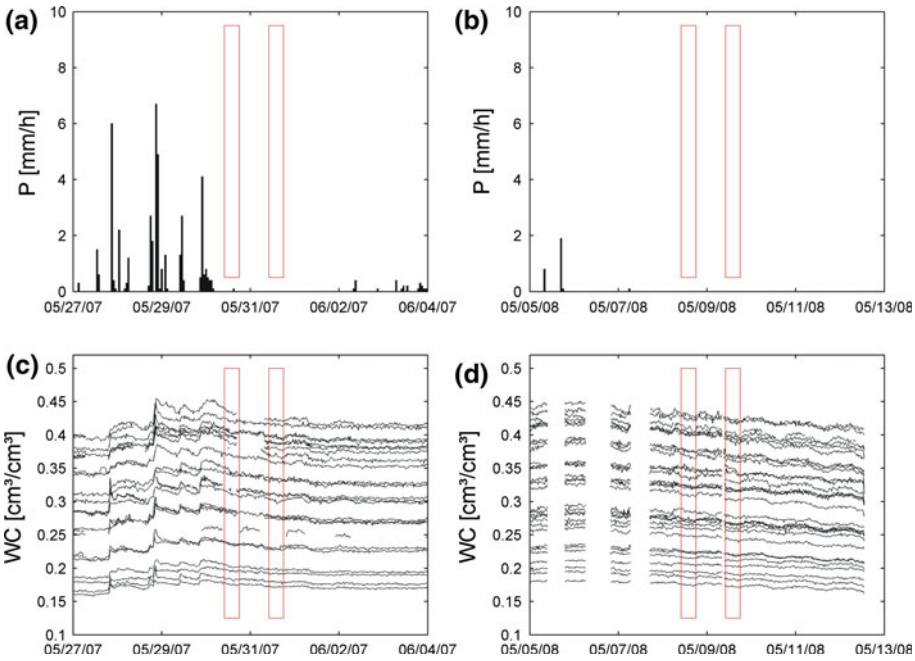

Fig. 6 Observations from the STDR cluster pasture location: Precipitation (*above*) and vertically integrated soil moisture dynamics (*below*) some days before and after the measurement campaigns in 2007 (**a**, **c**) and 2008 (**b, d**). Each *line* in the plots **c** and **d** represent the recorded soil moisture of an STDR probe. The *red bars* mark the dates of the measurement campaigns

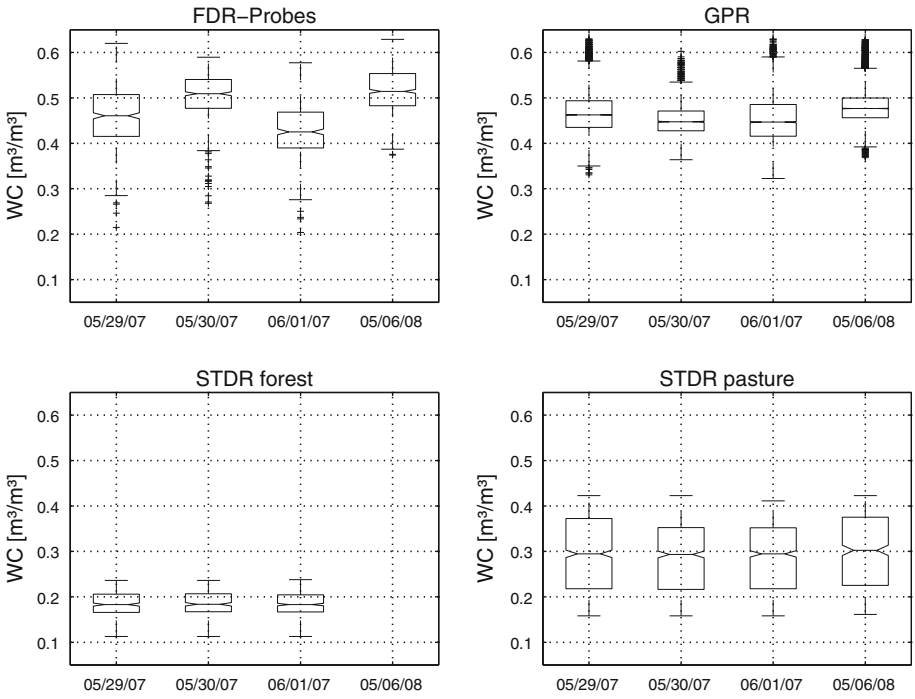

Fig. 7 Box plots of the measurements during the field campaign collected by FDR probes (*upper left*), GPR (*upper right*), and the STDR clusters 'forest' (*lower left*) and 'pasture' (*lower right*). The STDR data contain the depth-averaged values of each probe

on the same days are shown in the lower graphs. FDR and GPR data show higher water contents than the two STDR clusters. The data of the two clusters (pasture and forest) show relatively few variations on all 4 days. The FDR data show a wetting between May 29 and May 30, which may be due to a rainfall event of approximately 5 mm during that period. Afterwards, the data show a soil drying until June 1. The GPR and the STDR data do not reveal that kind of dynamic. These differences can be explained by the fact that FDR probes measure the upper soil layer only (6 cm), which is strongly affected by meteorological forcing. The GPR instrument measures to a depth of 8–12 cm depending on the soil moisture. And we assume that this depth experienced less wetting from the 5-mm precipitation event. The STDR cluster data are averaged values for the upper 60 cm soil layer, so the relatively small rainfall will hardly affect the mean value of this layer. The spatial soil moisture patterns observed by GPR are—at least partly—detectable in the results of the three individual GPR campaigns and also agree rather well with the results obtained from the other measurement techniques at this scale, such as FDR and the thermogravimetric method (not shown here).

3.1.3 FDR campaigns at different fields

The repeated measurements for soil moisture by FDR (Theta probes) in different fields during the campaign in spring 2008 permit the data analysis under two different aspects: the temporal dynamics and the spatial comparison of moisture characteristics for different fields at specific dates. Within a certain crop (see Table 2), e.g. winter wheat, we observed

Table 2 Results of soil moisture and vegetation monitoring during the measurement campaign from 24th April to 16th May 2008

Date	Water content (m^3/m^3)	Dry biomass (g/m^2)	Vegetation height (cm)	Canopy coverage (%)	Water content (m^3/m^3)	Dry biomass (g/m^2)	Vegetation height (cm)	Canopy coverage (%)	Water content (m^3/m^3)	Dry biomass (g/m^2)	Vegetation height (cm)	Canopy coverage (%)
	Winter wheat				Winter rye				Winter triticale			
24th April	0.28	12	7	9	0.30	17	7	16	0.37	10	8	17
03rd May	0.24	16	10	26	0.26	26	15	17	0.30	29	16	35
10th May	0.19	23	13	48	0.20	26	17	35	0.20	51	25	57
16th May	0.13	98	18	75	0.13	102	50	40	0.12	154	30	75
Date	Water content (m^3/m^3)	Dry biomass (g/m^2)	Vegetation height (cm)	Canopy coverage (%)	Water content (m^3/m^3)	Dry biomass (g/m^2)	Vegetation height (cm)	Canopy coverage (%)	Water content (m^3/m^3)	Dry biomass (g/m^2)	Vegetation height (cm)	Canopy coverage (%)
	Winter barley				Winter rape				Grassland			
24th April	0.22	47	9	27	0.32	194	18	63	0.43	126	11	73
03rd May	0.22	40	17	35	0.28	226	46	77	0.39	157	17	90
10th May	0.11	106	25	56	0.18	304	90	80	–	224	20	95
16th May	0.11	219	45	59	–	–	–	–	–	–	–	–
Date	Water content (m^3/m^3)	Dry biomass (g/m^2)	Vegetation height (cm)	Canopy coverage (%)	Water content (m^3/m^3)	Dry biomass (g/m^2)	Vegetation height (cm)	Canopy coverage (%)	Sites defined as bare and used in empirical relationship for estimation of soil moisture from ASAR data (see chapter 3.3)			
	Oats				Maize							
24th April	0.34	0	0	0	0.27	0	0	0	barley, rye, wheat			
03rd May	0.30	1	2	0	–	0	0	0	oats, barley, rye, wheat			
10th May	0.25	3	6	1	–	0	0	0	oats, rye, wheat			
16th May	0.20	8	9	13	0.18	0	0	0	oats, maize			

a continuing decrease in the soil moisture. From a rather high value of 27.6 Vol% (volumetric water content) at 24th April 2008, despite occasional precipitation events during the campaign, the soil moisture decreased to 12.6 Vol% (16th May 2008). The warm and dry weather period starting from the beginning of May amplified the rapid drying of the surface at the end of the campaign. The comparison of measurements made for different crop types on a single date (e.g. at 24th April 2008) reveals a spatial range in moisture from 22 to 42 Vol%. In particular, the fields which are already covered with relatively dense grass vegetation show high soil moisture values, which can be explained by the canopy acting as a kind of insulation against soil evaporation while plant transpiration is still very low at the beginning of the vegetation period.

The plant growth status (see Table 2) has a crucial influence on the estimation of soil moisture by remote sensing radar methods. Depending on the crop type, this influence is very small at the beginning of the campaign and increases with the growth of the plants. Thus, the dry biomass of winter wheat increased clearly in the observed weeks; it rose from 12 g/m^2 to approximately 100 g/m^2. In the same period, the plant height rose from 7 cm to 18 cm and the canopy coverage increased from 9 to 75%. In contrast, the soil surface roughness (summarising the geometrical features of the soil surface as boundary condition for the radar wave), the other influential parameter for radar-based soil moisture estimation, is stable over the period. Therefore, the roughness does not influence the backscatter–soil moisture relationship on the campaign days.

3.2 Small catchment scale: airborne multi-polarization microwave sensing

In order to achieve a reasonable soil moisture inversion in the case of vegetation-covered surfaces, the complex SAR scattering signal and the interacting scattering phenomena need to be analysed. The vegetation height of agricultural crops can reach a height of up to approx. 2 m and can have a strong vegetation orientation. In this case, the electromagnetic wave is propagating into the vegetation volume and has interactions with (a) the surface (surface scattering), (b) the surface and the stalks (dihedral scattering) and (c) with the volume (volume scattering) itself. Depending on the transmitted polarisation and wavelength, the electromagnetic wave propagates more or less strongly into the volume. Therefore, the main task in processing multi-frequency microwaves is to separate the different scattering contributions in order to decouple the volume component from the surface and the dihedral scattering contributions of the ground components. One promising way to separate the volume component from the ground component is the use of polarimetric diversity. SAR polarimetry is sensitive to the dielectric constant and the geometry of an illuminated object and is therefore able to distinguish different scattering mechanisms occurring within one resolution cell. The scattering object can be described by four elements of the transmitted and the received vector waves in horizontal (H) and vertical (V) polarisation, resulting in the following elements: HH, HV, VV and VH. Hence, the complex scattering matrix has five (3 amplitudes and 2 phases) independent parameters that can be used for physical parameter inversion. The polarimetric decomposition and inversion algorithm mentioned in Sect. 2.2.3 was applied on the L-band data set, recorded on the 30th/31st May 2007 by the DLR's E-SAR sensor. The conversion of the electrical permittivity into soil moisture is conducted with the same site-specific petro-physical model used in the processing of the TDR and GPR signals before.

Figure 8a shows the results of the different decomposition methods for the data of 31st May 2007. The different decomposition methods, their areal fraction and the assigned colours are listed in the legend to Fig. 8a. About 50% of the orientation cases can be

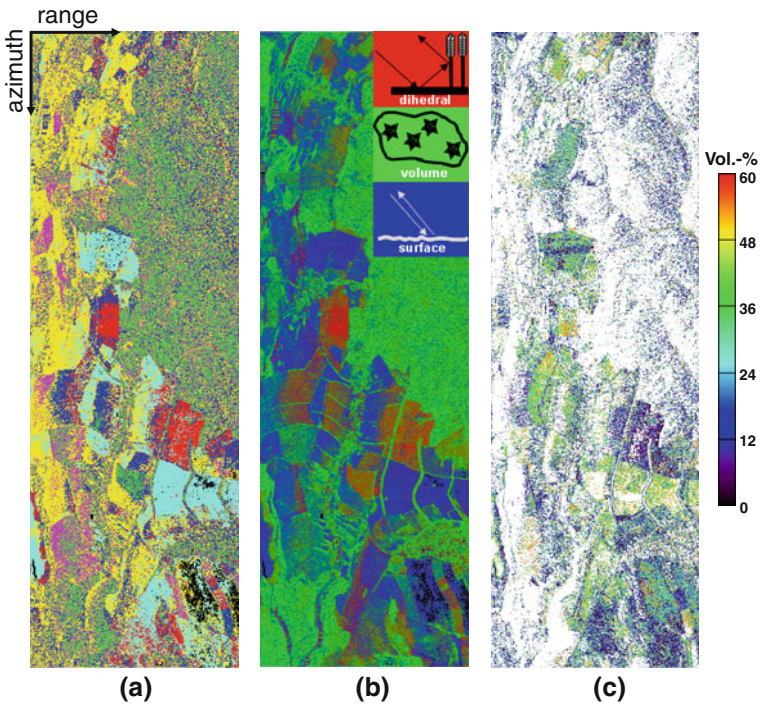

Fig. 8 **a** Map of different decomposition methods; **b** result of model-based three-component decomposition (*red*: dihedral scattering, green: volume scattering, *blue*: surface scattering); **c** estimated soil moisture from all inversion approaches. *White colour* represents non-invertible pixels (averaging window: 4 × 4)

assigned to random orientation (blue and yellow colours in Fig. 8a). Here, a major part of the dihedral dominant (21%) areas are located in the forested regions on the upper right of the image, while in the surface-dominant case (31%), the regions are located in areas with steep incidence angles. Further, 18% of the pixels have a vertical oriented volume and a dihedral scattering dominance. Therefore, these areas are mainly assigned to the forested areas and demonstrate the reasonable separation of the different scattering scenarios using the developed approach.

In Fig. 8b the normalised result of the model-based three-component decomposition is depicted as an RGB image, whereas the dihedral component is set to red, the volume component is set to green and the surface component is set to blue. The volume-dominated areas in green are clearly visible in the forested regions as well as in the urban areas. On the agricultural fields, the dihedral and surface components dominate compared with the volume component. Whether a field appears to have a dihedral or surface-dominant scatter depends on whether the field is already covered with a distinct vegetation layer or is still almost bare.

Figure 8c presents the estimated soil moisture for all applied decomposition methods merged in one image. The soil moisture ranges from 0 to 60 Vol%, whereas white areas are non-invertible. Compared with the model-based decomposition (Fig. 8b), the soil moisture inversion in the areas with dominant volume scattering (mainly forests: strong green colour) reveals rather sparse soil moisture results, which can be explained by the deficient modelling of the complex forest scattering. In addition, the near-range areas along the

Table 3 Vegetation parameters and measured (FDR) and estimated (SAR) soil moisture values at the three fields, respectively, recorded during the field campaign 30th/31st May 2007 (statistical parameters: field-averaged values, root mean square error (RMSE), standard deviation within each field (STDV))

	Vegetation parameters			Soil moisture (Vol%)			
	Plant height (cm)	Row distance (cm)	Wet biomass (kg/m^2)	Average value		RMSE	STDV
				Measured	Estimated		
Winter triticale	85	10	3.34	29.8	32.5	8.0	12.6
Field grass	27	10	1.13	32.0	36.8	9.9	10.6
Maize	16	75	0.1	27.0	31.2	9.5	14.2

azimuth direction also show a reduced inversion density arising from the steep slopes down to the Weisseritz river, which results in an almost perpendicular incidence angle (<20°), where the sensitivity to polarimetry is strongly reduced. For the agricultural fields, mostly located in the centre of the image, the inversion is quite homogenous especially on the less-vegetated fields (coloured in cyan in Fig. 8a), representing a horizontal volume with an underlying surface scatter.

A statistical comparison of the remotely sensed soil moisture estimates with the ground measurements from the FDR probes is given in Table 3 for three different land cover types. For the determination of the remotely sensed soil moisture estimates, 13 × 13 pixels around the ground sampling points were analysed, and the invertible pixels used for averaging. Only boxes with at least 25% of invertible pixels were considered to avoid outlier problems. The correlations between measured and estimated values for the three different fields (winter triticale, field grass and maize) exhibit a RMSE between 8.0 and 9.9 Vol%. Table 3 also shows key characteristics of the different crops, illustrating that the vegetation height differs between 16 and 85 cm and the wet biomass ranges from 0.1 to 3.34 kg/m^2. The STDV varies from 10.6 to 14.2 Vol% and therefore indicates a rather high variability at the subfield scale, both the backscattering patterns and/or the soil moisture itself. In addition, the mean 'ground-measured' (by FDR sampling) and 'mean remotely sensed' values (by SAR estimates) are given, with a maximum bias of 5 Vol%. Hence, the performed inversion of the mean surface soil moisture of the agricultural fields seems to be robust in the range of about 5 Vol%.

3.3 Extrapolation to larger catchments: satellite remote sensing of active microwaves

The ground measurements of soil moisture and canopy density (see Table 2) formed the basis to derive the empirical relationships between ground-measured and the satellite-based data for the 2008 field campaign. As long as the ground is not covered by dense vegetation, the derivation of this relationship is straightforward. However, it is obvious that the ASAR data from the densely covered grassland site are of little use to derive a profound relationship with the soil moisture of that field, and thus, the fields covered by grassland were not considered. A similar situation was experienced for the fields covered with winter rape, where the high canopy surface roughness disables the derivation of a profound correlation with soil moisture. Based on empirical experiences, we considered 50% of soil coverage or 100 g/m^2 of dry biomass as an upper limit for which a profound correlation function from reflecting signal (ASAR) and ground-measured moisture (by FDR) could be

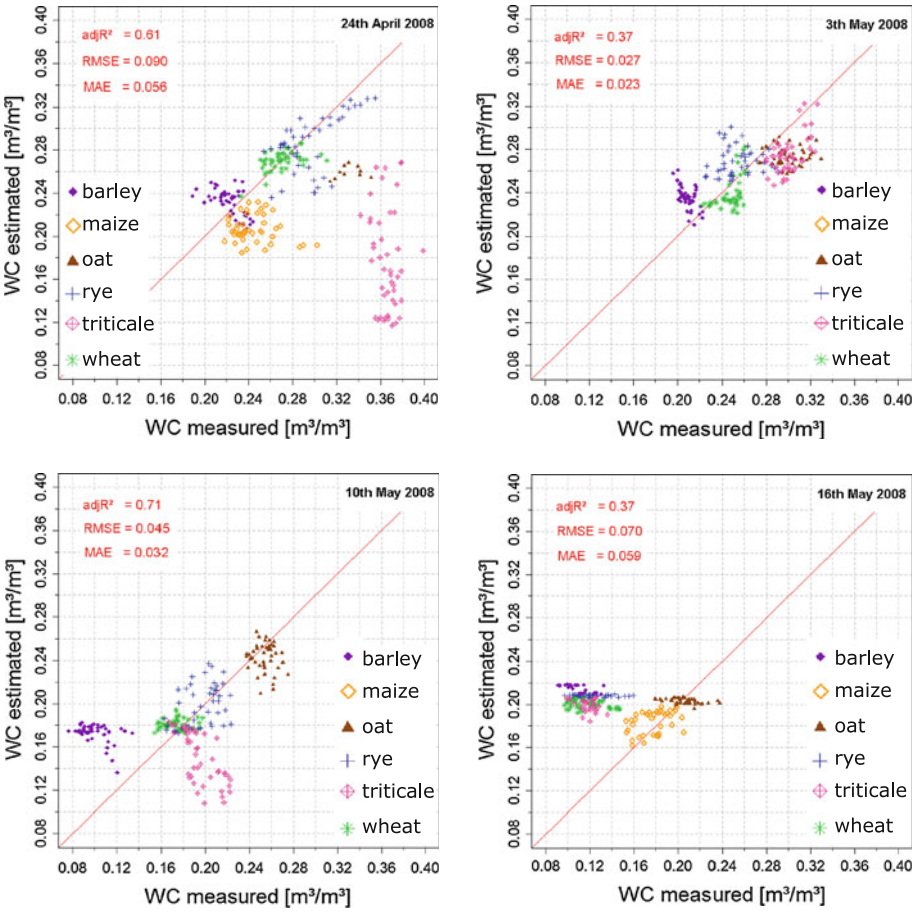

Fig. 9 Correlation plots between ground-measured and satellite-based (estimated) water content for aggregated ground measurements with different crop types based on one common function for the four dates of the measurement campaign. RSME and MAE are derived from all measurement data (training and validation sets), adj R^2 is based on each specific empirical relationship

determined. The fields with a vegetation cover below this limit value were defined as 'bare plots' and used to derive the correlations functions.

The resulting correlation plots for all the surfaces studied, except grassland, are shown in Fig. 9. One can see a reasonable correlation between the ground-measured values and the satellite data at all four dates for the bare surfaces such as rye at 24th April, wheat at 3rd May and maize at 16th May. The poor correlation for triticale at 24th April is to be explained on the one hand by the high soil moisture of approximately 40 Vol% (Baghdadi et al. 2006) and on the other hand by the high roughness of this particular field, where boars had rumpled the surface intensively. The fields where the vegetation height and density increased during the course of the ground measurement campaign are characterised by a decreasing correlation, such as triticale and winter barley at the first measuring date and later on all winter crops. By 16th May, only the summer crops of maize and oats can be estimated satisfactorily by satellite; for all other test fields the higher canopy density interfered with the backscattering which resulted in a clear overestimation of the moisture.

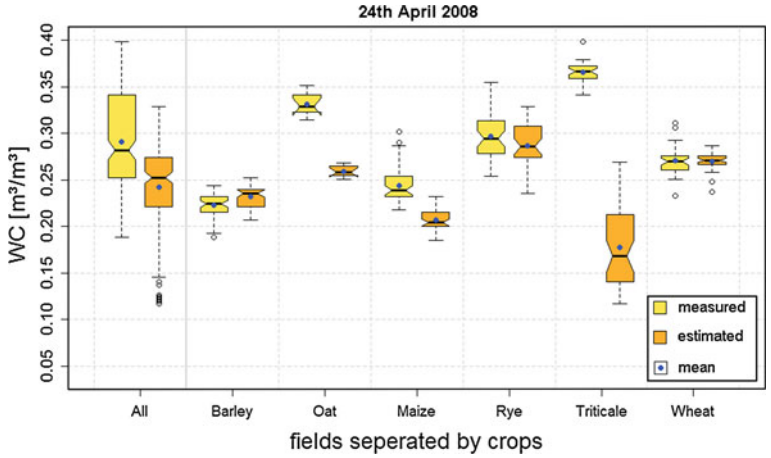

Fig. 10 Box-whisker plots for the water content estimated from ASAR data ('estimated') and from ground measurements ('measured') at 24th April 2008

In Fig. 10 and Tables 4 and 5 the statistical properties of the soil moisture data observed from space and from the ground are compared. One can see that for April 24, satellite-based and ground-measured data of winter wheat, winter barley and winter rye show similar statistical features. Table 5 shows that the high accuracy of the satellite-based data for the wheat test site lasts until May 10 (RMSE approx. 1 Vol%), and that by May 16, the high vegetation density decreases the performance (RMSE 8.3 Vol%). The statistical results for triticale reveal a large difference between ground- and satellite-based data, which is due to the unusual surface roughness of that field, as explained before. A similar difference is recorded for maize and oats. While for maize the remarkable roughness due to the typical land management (ploughing before sowing creates a furrow structure of 15 cm broad strips with micro-elevation differences of 10 cm) might be a cause of the under-estimation from space, no clear explanation for the underestimation could be identified for the oat test field. Despite the limitations discussed, it is worth noting that the mean soil moisture of all measured test sites (average of all ground data: 28 Vol%) is determined with an error less than 3 Vol% (average of all data from the satellite: 27 Vol%). This accuracy still holds for May 3 (26 Vol% vs. 27 Vol%) and for May 10 (18 Vol% vs. 19 Vol%). By May 16, however, the difference increases to 7 Vol% (13 Vol% vs. 20 Vol%) due to the increased vegetation cover.

Figure 11 displays the dynamics and the spatial distribution of the soil moisture of the agricultural fields during the measurement campaign, all determined from the four ASAR datasets. One can see that the moisture decreases from the first to the third date and also the erroneous increase from the third to the fourth date because of the soil moisture overestimation due to the increased vegetation cover. It should be noted that the soil moisture of winter rape fields in particular (e.g. coloured red in the third image) is not estimated correctly at all dates, because the vegetation cover is rather dense, even at the beginning of the measurements. The same comment is valid for the grassland areas, as explained above. For all other winter and summer crops, the derived correlation between ground and satellite data is considered to be reliable until the 3rd date (May 10). At May 16, only the fields of maize, oats and summer barley (pink, magenta and dark-green in the land use map) are

Table 4 Statistical properties for the water content [m^3/m^3] estimated from ASAR data ('e.') and from ground-measured data ('m.') at 24th April 2008, corresponding to Fig. 10

	All		Barley		Oat		Maize		Rye		Triticale		Wheat	
	m.	e.	m.	e.	m.	e.	m.	e.	m.	e.	m.	e.	m.	e.
Mean	0.282	0.236	0.223	0.232	0.331	0.259	0.244	0.207	0.297	0.286	0.366	0.172	0.271	0.270
Variance	0.276	0.218	0.018	0.014	0.014	0.003	0.034	0.016	0.062	0.069	0.011	0.219	0.022	0.008
RMSE	0.090		0.024		0.073		0.044		0.026		0.195		0.013	
MAE	0.056		0.021		0.072		0.037		0.020		0.188		0.010	

Table 5 Changes in statistical properties for the water content [m^3/m^3] estimated from ASAR data ('e.') and from ground-measured data ('m.') on the winter wheat test field during the four dates of the spring 2008 measurement campaign

	24th April		03rd May		10th May		16th May	
	m.	e.	m.	e.	m.	e.	m.	e.
Mean	0.271	0.270	0.248	0.239	0.174	0.181	0.118	0.200
Variance	0.022	0.008	0.010	0.022	0.012	0.003	0.023	0.001
1st quartile	0.261	0.267	0.010	0.022	0.012	0.003	0.106	0.197
2nd quartile	0.270	0.271	0.251	0.233	0.174	0.181	0.114	0.200
3rd quartile	0.276	0.276	0.254	0.241	0.180	0.184	0.129	0.203
Min. value	0.233	0.237	0.223	0.221	0.155	0.173	0.097	0.192
Max. value	0.311	0.286	0.261	0.283	0.197	0.194	0.147	0.206
RMSE	0.013		0.016		0.014		0.083	
MAE	0.010		0.013		0.012		0.082	

covered with somewhat sparse vegetation, which allows the relationship of backscattering signal and soil moisture to be applied reliably.

4 Simulation experiments on the influence of pre-event soil moisture on flood simulation

As described in the introduction, a major motivation for the multi-scale soil moisture observations is to investigate and evaluate the potential for further use in modelling catchment hydrology or even flood forecasting (Fig. 3). The requirements for such a model are as follows:

- It has to work in a distributed manner to be able to account for the spatially distributed soil moisture information, as well as the spatial data of land use and topography;
- It has to account for the governing hydrological processes, and—in the case of flood simulation—for flood-generating processes, which in the Weisseritz area are saturation excess overland flow and fast reacting subsurface flow mechanisms such as quick ground drainage flow and eventually subsurface stormflow (see Figs. 1, 2);
- It should provide a flexible model structure and an efficient coding to enable the integration of soil moisture data into the simulation process and to perform sufficiently fast model runs.

4.1 Short description of the model used

Based on these considerations, the hydrological model WaSiM-ETH, which is a modular, deterministic, process-oriented and distributed model for meso-scale catchments (Klok et al. 2001; Gurtz et al. 2003), has been selected. It was adapted and further applied to the Weisseritz catchment upstream of the gauge at Ammelsdorf, see Fig. 4. The chosen spatial discretisation is 100 m, the simulation time step 1 h, which is considered small enough to enable an appropriate representation of the governing flood runoff mechanisms. Rainfall data in hourly resolution were taken from five available meteorological stations within and nearby the catchment, spatially interpolated by inverse distance weighting.

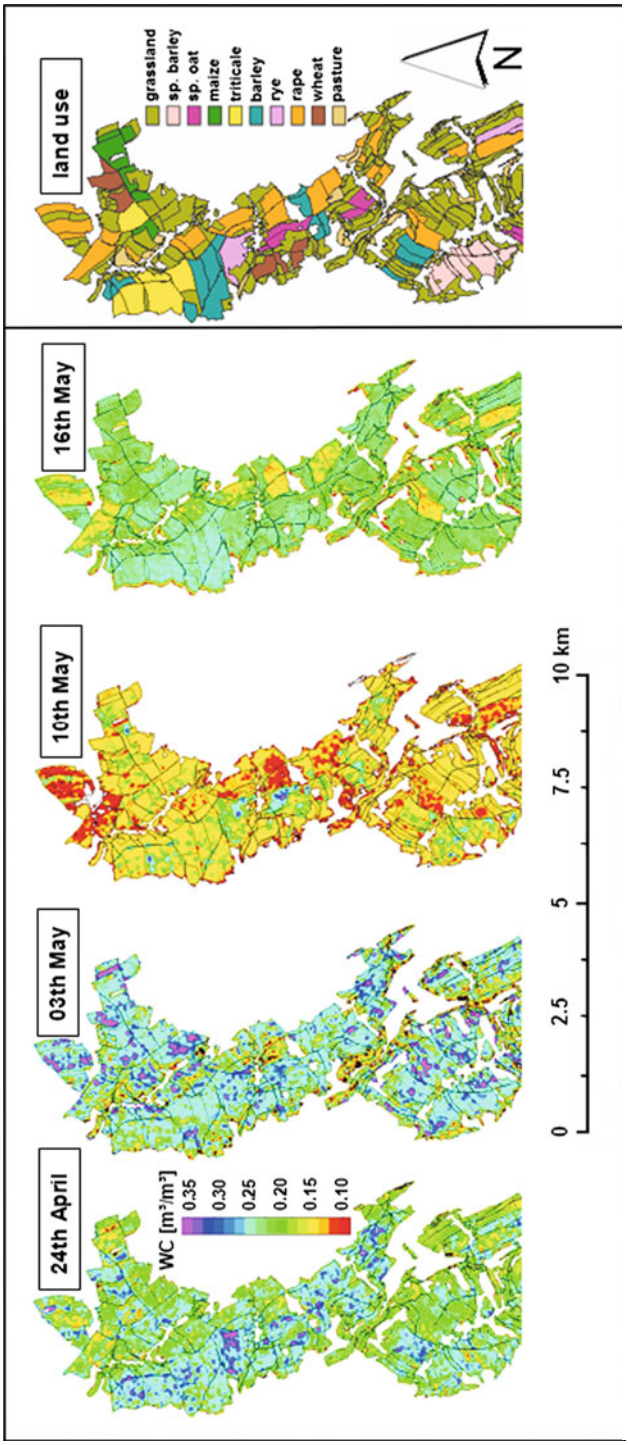

Fig. 11 Maps of temporal dynamics and spatial distribution of water content for the agricultural fields in the central part of the Weisseritz catchment, estimated from ASAR data at four dates. The *right-hand map* shows the land use of that area

WaSIM-ETH offers various options to represent soil moisture stores and fluxes (Schulla 1997; Schulla and Jasper 2007). We used the version, where the unsaturated zone water fluxes are described in a simplified manner, by conceptually distinguishing three different subsurface water storages: (a) *field capacity unsaturated* storage, (b) *gravitational (above field capacity) unsaturated* storage and (c) *saturated* storage. The field capacity unsaturated storage is vertically subdivided into the root zone and the below-root zone, where the water in the root zone represents the *plant available store (PAS)*. When infiltration into the soil occurs (which is calculated in a preceding step), water fills the field capacity unsaturated storage if free pore space is still available (non-saturated conditions). Otherwise, the infiltration water enters the gravitational unsaturated zone. The gravitational unsaturated zone storage either generates interflow (which exfiltrates into the river system) or percolates into the saturated zone storage. The exfiltration from the saturated zone storage forms the baseflow. Total runoff is composed from surface runoff (either by exfiltration overland flow or by saturation overland flow), interflow or baseflow.

Surface flow and interflow, as well as the unsaturated zone storages, are simulated for each grid cell, while the saturated zone storage and the resulting baseflow are calculated in a lumped manner on subcatchment level. The actual moisture conditions of the whole catchment are calculated continuously by the overall saturation deficit representing the catchment-wide difference between full catchment saturation (all stores filled) and the actual moisture. This overall saturation deficit is calculated for each time step, and its distribution within the catchment (i.e. the local saturation deficit at each grid) is estimated indirectly from the so-called soil-topographic index (Beven and Kirkby 1979). This means that not all soil water fluxes are simulated explicitly for each grid cell. This simplification yields quite fast simulations which explains the meso-scale potentials of this model, e.g. for flood-forecasting purposes. Process approaches for interception, evapotranspiration, infiltration, snow melt and streamflow dynamics are also included, see (Schulla and Jasper 2007) for details.

The model was calibrated for the 2-year period from summer 2000 until summer 2002, by the application of a Monte Carlo approach to provide 400 parameter-ensembles (within an adequate parameter space which was determined by preceding tests) from which the best-performing parameter combination was selected. Using observed discharge at the Ammelsdorf gauge, the Nash–Sutcliffe efficiency (NSE) for the calibration period was NSE = 0.61. For model validation, the period June 2002 to April 2006 was chosen, where a corresponding NSE was 0.14. This low value can be attributed to bad performing simulations of snow melt events during the validation period. For the subsequent analysis of flood modelling, we therefore focused on rainfall-triggered flood events (i.e. not triggered from snow melt) with a peak discharge of >1 m^3/s, yielding a total number of 8 events for further analysis, two of which are presented below.

4.2 Sensitivity analysis of simulated flood discharge to soil moisture

To assess the sensitivity of simulated flood runoff to soil moisture, simulation experiments were conducted for a series of storm rainfall events. The soil moisture conditions at the beginning of each flood event were taken from continuous simulations. For each simulation experiment, one of the three storages (a) plant available storage, (b) gravitational unsaturated storage and (c) saturation deficit (conceptually related to the saturated storage) were (1) increased by maximum 10% (if free pore space available) or (2) decreased by 10%. This yields a total number of seven simulations for each event: one unmodified and six modified initial water content conditions. We consider these scenarios as physically

plausible because the values of increase/decrease are chosen to be within the physical range of soil moisture, the increase has been limited by an upper bound (i.e. saturation) and only one storage per scenario was modified in order not to generate increase in moisture in one storage and decrease in another one. Table 6 gives an overview of the actual values of the water contained in the three different model storages and the modifications for two selected rainstorm-triggered flood events in June 05 (total precipitation: 133 mm) and September 2007 (total precipitation: 96 mm). It is important to understand that the model's plant available storage (obtained from the continuous simulations) is almost filled at the beginning of the two events (182 mm and 170 mm, which corresponds to 99.9 and 92% saturation, respectively). That is why a further increase is hardly possible (only 0.01 mm and 5.3 mm, respectively).

Figure 12 presents the results for the simulation experiments for the two selected events. As expected, an increase in storage filling leads to an increased discharge. WaSiM-ETH reacts rather sensitively to the 10% reduction (18 mm) in the PAS (e.g. up to more than 2 m^3/s in the left panel of Fig. 12). This model feature can be attributed to the high water content in the PAS as explained before. As flood generation processes such as saturated overland flow and subsurface storm flow become active only if the PAS is saturated, a reduction in PAS content explains the high model sensitivity. The model sensitivity is moderate towards changes in the saturated storage and changes in the gravitational zone storage.

4.3 Using observed soil moisture for flood simulation

In order to assess the potentials of pre-event soil moisture data for flood modelling, we tested the satellite-based data (as described in Sect. 3.3) as initial conditions for the

Table 6 Initial soil moisture values (spatial averages) for the simulation experiments of the flood events in June 2005 and September 2007

	June 2005			September 2007		
	Unmodified (mm)	Increase (mm)	Decrease (mm)	Unmodified (mm)	Increase (mm)	Decrease (mm)
Plant available storage	182	0.01	−18	170	5.3	−17
Unsaturated zone	6	0	−0.4	19	0.3	−1.7
Saturation deficit	52	5	−5	69	7	−7

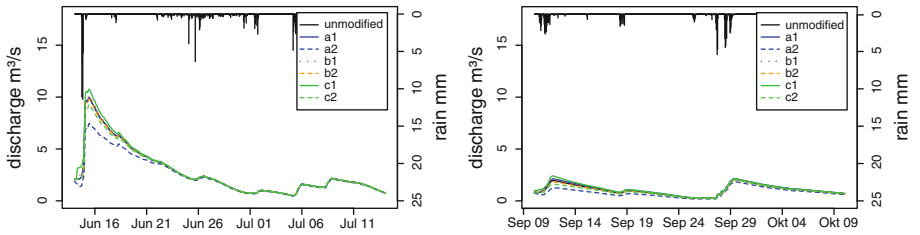

Fig. 12 Results from simulation experiments for two selected events in June 2005 (*left*) and September 2007 (*right*) assessing the sensitivity of the WaSiM-ETH model to changes in initial conditions in the three storages (*a*) plant available store, (*b*) unsaturated zone and (*c*) saturation deficit with 10% increased (*1*) or decreased (*2*) storage content

simulation of flood events. In general, we aimed at directly incorporating the observation values in the initial conditions to be provided for the flood modelling procedure. Even though the utilisation of how to use soil moisture data for the modelling procedure seems to be straightforward, there are some important problems constraining their operational value:

1. The sampling depth of the observations is different from the depth relevant for flood generation processes. In particular, the dynamics of the soil moisture in the saturated zone (e.g. the groundwater) can be highly relevant for flood generation but remote sensing methods are unable to capture the groundwater state.
2. Even satellite or airborne systems may not deliver soil moisture observations covering the whole catchment, due to only partial coverage of the catchment (in case of the airborne system) or due to difficulties with areas covered by dense vegetation (see Sects. 3.2 and 3.3) Thus, the missing data have to be estimated by interpolation or regionalisation (transfer) methods from the measured values.
3. Even if soil moisture data would be available or could be estimated for the entire catchment area, those values might be difficult to apply to many rainfall-runoff models, because these models rarely use direct and spatially distributed soil moisture values, usually using more conceptual types of soil moisture information such as filling of storage functions. The transfer of the observed values into the model parameters is not a trivial task and not unequivocal.

Instead of applying the actually recorded, very little rainfall amount following the period after our measurement campaigns, we used two previously recorded heavy rainfall periods of 1 month duration (total rainfall of the 1st period: 161 mm; total rainfall of the 2nd period: 156 mm) as precipitation input for the simulation of scenario-type flood events. As initial soil moisture conditions we used:

1. The satellite-based soil moisture observations from 24th April 2008. The spatially averaged observation values was 27 Vol% (see Table 5), which is equivalent to a relative moisture value of 71%. These spatially distributed observation values were prescribed for both the plant available storage and the gravitational unsaturated storage. In case satellite-based values were not available (such as for most of the forested areas), we used as a uniformly distributed proxy the average value measured at the STDR 'forest cluster'.
2. Soil moisture obtained from continuous simulations for 24 April 2008. The moisture of the plant available storage obtained by continuous simulation for that day had a value of 100% soil moisture, i.e. full saturation. The gravitational unsaturated storage had in average a filling of 10 mm, what corresponds to a relative soil moisture value of 17%, as the storage capacity at that day amounted in average to 60 mm.

It is important to realise that there exist three major differences between the two initial condition types: the total moisture value is different, the moisture is allocated differently to the two near-surface model storages and the spatial pattern is not the same. Hence, it is not surprising that the simulated flood hydrographs for these two different initial conditions show a clear difference in flood peak. In the case of the first simulated rainfall event (left part of Fig. 13), the peak discharge obtained by using the observed soil moisture is about 10 m^3/s compared with 14 m^3/s when using the initial conditions derived from continuous simulations. The second simulated rainfall event (right part of Fig. 13) yields a peak discharge of roughly 6 m^3/s when using the observed soil moisture as compared with 8.5 m^3/s when using the initial conditions derived from continuous simulations.

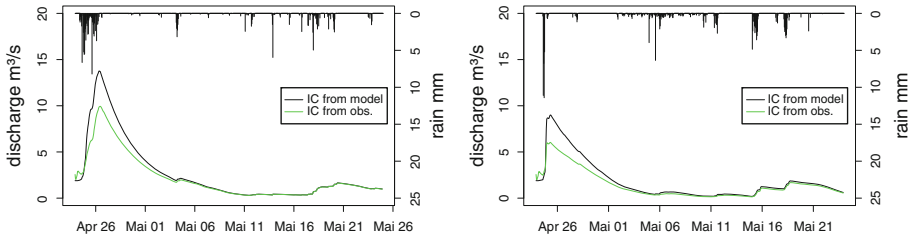

Fig. 13 Testing the influence of soil moisture on flood event simulations with scenario-type storm rainfall. *Left*: scenario rainfall no. 1 (total rainfall: 161 mm), *right*: scenario rainfall no. 2 (total rainfall: 156 mm). Initial conditions are from continuously simulated soil moisture values at the date of the sampling campaign (IC from model) as well as from satellite-based observed soil moistures from the sampling campaign (IC from obs.). More explanations are given in the text

Thus, one can clearly see that pre-event soil moisture conditions are of major importance for flood simulations. One has to be aware that neither the storage filling derived from the remote sensing nor the one derived from continuous simulation can be considered the 'right' one, as both bear method-specific uncertainties: the remote sensing data reflect water content only at the soil surface and besides do hardly contain any information in densely vegetated areas, such as forests. The soil moisture status derived from continuous simulation may better be able to represent the overall catchment response to rainfall. However, it requires model calibration, and therefore the thereby adjusted soil moisture storage values might be over- or underestimated to compensate for other model shortcomings.

5 Discussion

As outlined in the first section, pre-event catchment wetness is crucial for the runoff response to rainfall or snow melt events. Thus, it is an obvious aim to monitor this important catchment condition to improve the performance of runoff modelling, including floods. Our study has shown that there are a range of measurement methods available, from the conventional (e.g. thermogravimetric method) to innovative techniques (e.g. STDR, GPR and airborne SAR). It could be shown that it is possible to conduct measurement campaigns to record soil moisture at multiple spatial scales, different measurement depths and observation frequencies at least partially link the information derived from the different methods and scales. However, one has to be aware that such campaigns and application of novel technologies still require lots of efforts, time and manpower and thus can hardly be conducted for an operational real-time purpose, such as flood forecasting, today.

Besides these encouraging results, however, one has to deal with several constraints which limit the potential of the measurements for further use in flood modelling: (a) the different measurement methods are associated with various kinds of uncertainties; (b) the different measurement methods have limited coverage in space and/or time; (c) the various flood generation processes are influenced differently by soil moisture and (d) many hydrological models, including most forecasting models, are unable to incorporate soil moisture values directly.

5.1 Uncertainties and limitations of the tested soil moisture measurement methods

During the measurement and data processing procedures, one faces the following uncertainties:

- Uncertainties directly associated with the measurement method (measurement error);
- Uncertainties due to different spatial coverage, spatial resolution, measurement depth and observation frequency;
- Uncertainty due to the data processing, i.e. due to the transformation of the measured signal to a soil moisture value (e.g. electromagnetic model and inversion model).

In the following, we discuss these issues for the different spatial scales studied here.

5.1.1 Plot scale

The gravimetric measurement method is well known as a fairly accurate method, in terms of both measurement error and signal processing, e.g. if the sampled soil is rather homogeneous and the method is applied carefully, the resulting uncertainty can be below 2 Vol%. However, the use of this method is very limited, because one can neither retrieve soil moisture information covering meso-scale catchments nor repeat measurements at the same site. The FDR-based point measurements (by hand-held Theta probes) come with a total measurement uncertainty of at least 3–7 Vol% for the 2007 campaign and represent only the small-scale values, similar to the results from thermogravimetric measurements. Nevertheless, such measurements can be repeated at the same site (or even recorded continuously if connected to a data logger) and can be distributed over a couple of km^2 during measurement campaigns. One must also be aware that such field campaigns with hand-held FDR yield moisture data for the near-surface only (rod length 6 cm).

5.1.2 Field scale

As described in Sect. 3.1, the soil moisture at field scale was monitored by two STDR clusters (see Figs. 6, 7) and by GPR. In addition, field scale soil moisture was derived from spatially interpolated FDR data collected during the intensive measurement campaigns (see Table 1; Fig. 5). Figure 6 shows high small-scale spatial variability and temporal dynamic of soil moisture monitored with the STDR cluster. Thus, the main source of uncertainty of that measurement technique can be referred to the specific small sampling scale of that method and is reflected by a strong and almost random micro-scale spatial variability. These strong small-scale variations dominate the appearance of soil moisture patterns over the two monitored STDR cluster areas, as there was hardly any organised variability detectable.

The mean and the maximum of the standard deviations of the FDR measurements for three investigated agricultural fields have been calculated for the 2007 campaign. At all fields, the mean of the standard deviations of a sampling point was below 3 Vol% (2.6 Vol% for winter triticale, 2.3 Vol% for field grass, and 2.4 Vol% for maize, respectively), while the maximum of the standard deviations can reach 7 Vol% for some individual sampling points (6.0 Vol% for winter triticale, 4.5 Vol% for field grass, and 7.4 Vol% for maize, respectively). Hence, one has to acknowledge a measurement uncertainty of 3–7 Vol% for the point measurements by FDR.

The GPR measurements revealed a similarly strong small-scale variability as identified from the STDR clusters. However, the overall soil moisture showed a notably different

pattern compared with the one derived from the FDR measurements (not shown here). Besides differences in measurement errors, we attribute these differences to the different measurement depth of the two methods (6 cm for the FDR and approx. 8–12 cm for the GPR, respectively).

Referring to the measurement duration and frequency in time, it is evident that the STDR clusters collect continuous data as the individual STDR probes are connected to data loggers. Actually, in our study, the STDR method was the only one collecting continuous soil moisture data. GPR and FDR measurements are limited to the campaigns, as the GPR device needs to be drawn manually over the soil surface and the FDR probes have to be inserted manually into the chosen points distributed over the sampling area.

5.1.3 Catchment scale

As described in Sects. 3.2 and 3.3, the soil moisture at the catchment scale was monitored by airborne microwave remote sensing (small catchment scale) and by analysing ASAR satellite images (larger catchment scale).

The uncertainties of the airborne microwave remote sensing can be related to the *electromagnetic model* and to the *inversion model*, respectively: The concept of modelling a vegetation volume by means of polarimetry assumes a cloud of uniformly shaped particles with a certain orientation perpendicular to the incidence plane (Cloude et al. 1999). Hence, there are two parameters, the particle shape and the particle orientation, for which assumptions have to be made (Yamaguchi et al. 2005). These simplifications are necessary, but cause uncertainties that contribute to the bias of the presented results. In the inversion procedure, simple electromagnetic models are used to describe single components, which might not be adequate for the scattering of certain vegetation covers. Moreover, the modelled ground components are related to the decomposed ground components, which may introduce some additional uncertainties. It is not possible to quantify these uncertainties on their own, but one can compare the results with ground measurements (e.g. by FDR) and from there derive an uncertainty of roughly 3 Vol% in average and 7 Vol% maximum.

In Fig. 10 and Tables 4 and 5, the statistical properties of the satellite-based method have already been displayed. One must emphasise that this method still requires the simultaneous collection of ground data to derive an empirical relationship between ground data and signals monitored in space. If this relationship is known, ASAR data allow the estimation of soil moisture from the satellite data with an error lower than 3 Vol% for bare agricultural fields. For densely covered fields, the relationships are much more uncertain (10 Vol% or more), which strongly reduces the applicability of satellite data for such land cover. To allow an operational use of satellite-based radar data, further research needs to be performed deriving an universal relationship for all acquisition dates, taking into account the influences of vegetation cover and roughness. Upcoming satellite missions with L-band and polarimetric data will provide new opportunities based on the methodology shown in the Sect. 3.2. Today, the identification of the spatial distribution and temporal dynamics of soil moisture (e.g. analysing one satellite scene per week) is limited to bare sites.

Referring to the measurement duration and frequency in time, one must keep in mind that both the airborne and the satellite observations are available only for the dates of the over-flights, which restricts the availability of such data so far, e.g. not more than once or twice a plane flight a year and roughly one satellite scene per week, respectively. Therefore, continuous data from such systems, in particular from the airborne system, are not available. To really track the trend and the changes in soil moisture, a time series is

Table 7 Usability of the different measurement methods to capture soil moisture at the adequate coverage, space–time scales and accuracy required for three flood runoff generation processes influenced by soil moisture. The measurement accuracy is rated acceptable only if the required measurement depth can be achieved

Measurement method	Required areal coverage	Required measurement depth	Required measurement frequency	Required measurement accuracy
Flood-generating process: *Saturation excess induced overland flow (SO)*				
Thermogravimetric	No	Yes	No	Yes
Theta probe (FDR)	Yes[a]	Yes	No	Yes
STDR cluster	No	Yes	Yes	Yes[b]
Ground-penetrating radar (GPR)	No	Yes	No	Yes
Airborne polarimetric SAR	Yes[c]	Yes	No	Yes
Satellite Envisat ASAR	Yes	Yes	No	Yes[d]
Flood-generating process: *Subsurface stormflow (SSF)*				
Thermogravimetric	No	No	No	
Theta probe (FDR)	No	No	No	
STDR cluster	No	Yes[e]	Yes	Yes[e]
Ground-penetrating radar (GPR)	No	No	No	
Airborne polarimetric SAR	Yes	No	No	
Satellite Envisat ASAR	Yes	No	No	
Flood-generating process: *Quick groundwater drainage (GD)*				
Thermo-gravimetric	No	No	No	
Theta probe (FDR)	No	No	No	
STDR cluster	No	No	Yes	
Ground-penetrating radar (GPR)	No	No	No	
Airborne polarimetric SAR	No	No	No	
Satellite Envisat ASAR	No	No	No	

[a] In case many individual measurements (measurement campaign) can be performed

[b] But near-surface values unreliable due to uncertain inversion of measured signal

[c] For rather small catchment sizes (to be covered by a flight campaign)

[d] But ground calibration needed

[e] But extensive post-processing of data needed

necessary, which can represent weekly and seasonal fluctuations and thus might reveal critical catchment states.

The uncertainties and shortcomings of the different measurement methods constrain the value of such soil moisture values for an operational use, e.g. for flood forecasting. Here, it is worthwhile distinguishing the main three flood runoff generation processes: Saturation excess–induced overland flow, subsurface stormflow and quick groundwater drainage, as explained in the introduction (Fig. 2). Table 7 summarises the usability of the soil moisture data resulting from the different measurement methods. For the applied technologies, the measurement accuracy is not the most constraining problem. Instead, it is obvious that there is no method that can deliver on its own all the necessary spatial and temporal information, in area, depth and frequency.

The generation of saturation excess induced overland flow (OF) depends on the presence of saturated areas at the soil surface. Thus, for this process, it is sufficient to have

information on the direct surface conditions available, obtained from all measurement methods. The areal coverage can be gained from the remote sensing methods and/or by FDR measurement campaigns. However, continuous measurements can be collected only from a ground-based system connected to a data logger (in our case the STDR clusters), which does not allow for spatial coverage at the catchment scale.

Subsurface stormflow (SSF) might occur in the case of occasionally saturation in a well conductive sloping layer overlying a zone of little or no permeability and corresponding lateral preferential flow phenomena. That means that the identification of SSF-favourable catchment conditions requires soil moisture information through the soil down to layers of reduced permeability, which might be at least to a depth of approx. 1 m to 2 m, with a dense resolution in space and time. With the exception of the STDR cluster, none of the systems can deliver a measurement depth relevant for that process. Even the STDR cluster cannot deliver catchment-wide information, because of its restriction to a relatively small area (a few 100 m^2) and to a maximum measurement depth of 60 cm.

Quick groundwater drainage (GD) occurs in the case of a steep increase in the groundwater gradient, triggered by fast groundwater recharge processes, e.g. through preferential flow paths. Thus, GD occurrence might be guessed from direct groundwater table observations in space and time. As none of the measurement techniques applied in this study measure the groundwater gradient, GD cannot be assessed.

5.2 Limited usability of soil moisture data for flood modelling and forecasting

At a first glance, the idea of using soil moisture data to initiate better flood modelling (including flood forecasts) seems to be a rather straightforward approach. However, this approach also bears some technical problems regarding the operational use of such data and the model parameterisation. A main constraint is that the observation of spatially distributed soil moisture, and the subsequent data processing is still far from an operational stage because continuous or quasi-continuous airborne observation and processing of soil moisture (as presented in Sect. 3.2) are not available. Also, satellite data are not yet readily available continuously and in a way that they can be used directly for flood forecasting, see 3.3. In our case, only two dates with airborne soil moisture information were available (the results from one date are presented in Sect. 3.2). However, this date (which had to be fixed months ahead to enable the complex and costly measurement flight and the parallel ground campaign to take place) was not followed by a heavy rainfall. Thus, we cannot directly assess the usefulness of this measurement for the simulation of a real flood in a forecasting mode.

Last but not least, one has to acknowledge the limited readiness of many hydrological models to directly use soil moisture data. As demonstrated in Sect. 4, these difficulties are because most models rarely use spatially distributed soil moisture values as input, rather than the more conceptual type of soil moisture information such as the filling of storage functions as a state variable of the model. A transfer function may relate observed moisture to this state variable. However, the transfer of the observed values into such model variables is not unequivocal.

6 Conclusions and outlook

Basically, observed soil moisture data may improve the performance of operational rainfall-runoff models in three ways:

1. Soil moisture data can be used for model initialisation, possibly using a transfer function, which relates the observed moisture to a state variable of the model. Although continuous hydrological models need to be initialised as well, this is of primary importance in event-based modelling. In any case, moisture data need to be available for all spatial units (e.g. sub-basins) of the model at the date of initialisation.
2. Data on observed soil moisture may be exploited by assimilation techniques. Data assimilation aims at re-estimating model parameters or state variables using the latest observations. Again, if a distributed hydrological model is used, moisture data must be available for all spatial units.
3. Observed time series of soil moisture may be used in conjunction with hydrographs to calibrate the multiple parameters of a rainfall-runoff model or to verify its simulation results. In that case, spatial and temporal completeness of the data is not a prerequisite. However, it is crucial that the observations actually represent the corresponding spatial units of the model and, as always, the relation between observations and a model's state variable must be known.

Having these three potential uses of soil moisture observations in mind, the following results of our study seem to be important:

- The satellite radar data tested are frequently, but not continuously, available and cover a large area with high spatial resolution. However, they allow for a reliable estimation of bare-soil moisture only. For areas with a significant vegetation cover (which may be $> 80\%$ of the catchment before harvest), soil moisture data of sufficient quality cannot yet be retrieved. In contrast, the airborne radar data do appear suitable for estimating the average soil moisture in the top soil for the crop-covered areas tested. However, similar to the satellite approach, no data may be collected for a considerable part of the catchment, which is covered by forest. Generally, airborne radar data do not require simultaneous ground measurements but are not operationally available. In summary, both kinds of the remotely sensed data can hardly be used for initialising a distributed hydrological model or for the purpose of operational data assimilation.
- The ground-based measurements of soil moisture using TDR/FDR, GPR, STDR and the thermogravimetric approach revealed a high spatial variability at the point scale, the plot scale, and also the hillslope scale. Furthermore, the agreement between the different methods with respect to absolute values of the moisture is rather low. Consequently, it is difficult to compare soil moisture data measured at a single point, plot, or hillslope with simulated values taken from a meso-scale hydrological model. Also, one must expect large errors when point data are regionalised by geostatistical approaches. The high correlation of the soil moisture time series recorded at the single probes of STDR clusters suggests that a comparison of measured and modelled soil moisture data should focus on the dynamics but not on absolute values.
- The STDR clusters equipped with a data-logging system were the only system in our study capable of recording continuous data. Thus, in terms of achieving a reasonably comprehensive picture of soil moisture in space and time, a combination of local but continuous measurements, with techniques covering rather large areas (remote sensing), is recommended.

It has to be realised that, in spite of innovative measuring techniques at all spatial scales, soil moisture data for entire vegetated catchments are still not operationally available yet. Therefore, we suggest that observations of soil moisture should primarily be used to improve the quality of continuous, distributed hydrological catchment models that simulate

the spatial distribution of moisture internally. Thus, when and where soil moisture data are available, they should be compared with their simulated equivalents in order to improve the parameter estimates and possibly the structure of the hydrological model. Depending on its spatial discretisation, such a comparison may require that ground-based measurements and remotely sensed data are combined to yield 'observations' on a spatial scale that is similar to the size of a model unit.

It was explained that river discharge and in particular flood events are composed from different runoff generation processes. Each of such processes is influenced by the soil moisture through different mechanisms. In this study, the recorded soil moisture was at the soil surface or near the soil surface. This information is important for saturated overland flow. In contrast, subsurface stormflow and quick groundwater drainage are related to deeper soil moisture or to the groundwater conditions, respectively. Until now, there is no technology readily available that could monitor subsurface stormflow in an operational manner. Concerning quick groundwater drainage, one might derive important knowledge by monitoring the groundwater level at selected observation wells of the upper groundwater layer (to be recorded continuously) and combine this information with expert knowledge of the spatial pattern of the groundwater table and its seasonal variations.

Acknowledgments This research has been conducted as part of the project OPAQUE (operational discharge and flooding predictions in head catchments), a project funded by the German Federal Ministry of Education and Research within the research programme RIMAX ('Risk Management of Extreme Flood Events'). This financial support is gratefully acknowledged, as well as the further funding of measurement equipment and technical support from the University of Potsdam and the GFZ German Research Centre for Geosciences. We thank Thomas Recknagel for conducting the WASIM-ETH simulations. Furthermore, we thank two anonymous reviewers for their clear and constructive comments to an earlier version of this paper.

References

Aubert D, Loumagne C, Oudin L (2003) Sequential assimilation of soil moisture and streamflow data in a conceptual rainfall-runoff model. J Hydrol 280:145–161

Baghdadi N, Holah N, Zribi M (2006) Soil moisture estimation using multi-incidence and multi-polarization ASAR data. Int J Remote Sens 27(10):1907–1920

Berthet L, Andréassian V, Perrin C, Javelle P (2009) How crucial is it to account for the antecedent moisture conditions in flood forecasting? Comparison of event-based and continuous approaches on 178 catchments. Hydrol Earth Syst Sci 13:819–831. doi:10.5194/hess-13-819-2009

Beven KJ, Kirkby MJ (1979) A physically based, variable contributing area model of basin hydrology. Hydrol Sci J 24(1):43–69

Blöschl G, Sivapalan M (1995) Scale issues in hydrological modelling: a review. Hydrol Proc 9:251–290

Borga M, Boscolo P, Zanon F, Sangati M (2007) Hydrometeorological analysis of the August 29, 2003 flash flood in the eastern Italian Alps. J Hydrometeorol 8(5):1049–1067

Brocca L, Melone F, Moramarco T, Morbidelli R (2009) Antecedent wetness conditions based on ERS scatterometer data. J Hydrol 364(1–2):73–87

Bronstert A (2005) Abflussbildung. Forum für Hydrologie und Wasserbewirtschaftung, Heft 12

Bronstert A, Bárdossy A (1999) The role of spatial variability of soil moisture for modelling surface runoff generation at the small catchment scale. Hydrol Earth Syst Sci 3(4):505–516

Bronstert A, Bárdossy A (2003) Uncertainty of runoff modeling at the hillslope scale due to temporal variations of rainfall intensity. Phys Chem Earth 28:283–288

Cassiani G, Binley A, Ferré TPA (2006) Unsaturated zone processes. In: Verrecken H, Binley A, Cassini G Revil A, Titov C (eds) Applied hydrogeophysics, NATO science series, IV. Eart and environmental sciences, vol 71. Springer, Dordrecht

Choi M, Jacobs JM, Cosh MH (2007) Scaled spatial variability of soil moisture fields. Geophys Res Lett 34:L01401. doi:10.1029/2006GL028247

Cloude SR, Pottier E (1996) A review of target decomposition theorems in radar polarimetry. IEEE Trans Geosci Remote Sens 34(2):498–518

Cloude SR, Pottier E (1997) An entropy based classification scheme for land applications of polarimetric SAR. IEEE Trans Geosci Remote Sens 35(1):68–78
Cloude SR, Fortuny J, Lopez-Sanchez JM, Sieber AJ (1999) Wide-Band Polarimetric Radar Inversion Studies for Vegetation Layers. IEEE Trans Geosci Remote Sens 37(5):2430–2441
Collier CG (2007) Flash flood forecasting: what are the limits of predictability? Q J R Meteorol Soc 133(622):3–23
Corwin DL, Hopmans J, de Rooij GH (2006) From field- to landscape-scale vadose zone processes: scale issues, modeling, and monitoring. Vadose Zone J 5(1):129–139
Crow WT, Ryu D (2009) A new data assimilation approach for improving runoff prediction using remotely-sensed soil moisture retrievals. Hydrol Earth Syst Sci 13(1):1–16
Crow WT, Bindlish R, Jackson TJ (2005) The added value of spaceborne passive microwave soil moisture retrievals for forecasting rainfall-runoff ratio partitioning. Geophys Res Lett 32:L18401. doi: 10.1029/2005GL023543
Dunne T, Moore TR, Taylor CH (1975) Recognition and prediction of runoff producing zones in humid regions. Hydrol Sci Bull 20(3):305–327
Ehret U (2003) Rainfall and flood nowcasting in small catchments using weather radar. Mitteilungen Institut für Wasserbau, Universität Stuttgart
Evett SR, Schwartz RC, Tolk JA, Howell TA (2009) Soil profile water content determination: spatiotemporal variability of electromagnetic and neutron probe sensors in access tubes. Vadose Zone J 8:926–941. doi:10.2136/vzj2008.0146
Fedora MA, Beschta RL (1989) Storm runoff simulation using an antecedent precipitation index (API) model. J Hydrol 112(1–2):121–133
Feng W, Lin CP, Deschamps RJ, Drnevic VP (1999) Theoretical model of a multisection time domain reflectometry measurement system. Wat Resour Res 35(8):2321–2331
Francois C, Quesney A, Ottle C (2003) Sequential assimilation of ERS-1 SAR data into a coupled land surface-hydrological model using an extended Kalman filter. J Hydrometeorol 4(2):473–487
Freeman A, Durden SL (1998) A three-component scattering model for polarimetric SAR data. IEEE Trans Geosci Remote Sens 36(3):963–973
Galagedara LW, Parkin GW, Redman JD, von Bertoldi P, Endres AL (2005a) Field studies of the GPR ground wave method for estimating soil water content during irrigation and drainage. J Hydrol (Amsterdam) 301:182–197
Galagedara LW, Redman JD, Parkin GW, Annan AP, Endres AL (2005b) Numerical modeling of GPR to determine the direct ground wave sampling depth. Vadose Zone J 4:1096–1106
Gaskin GJ, Miller JD (1996) Measurement of soil water content using a simplified impedance measuring technique. J Agric Res 63:153–160
Goodrich DC, Schmugge TJ, Jackson TJ, Unkrich CL, Keefer TO, Parry R, Bach LB, Amer SA (1994) Runoff simulation sensitivity to remotely-sensed initial soil water content. Wat Resour Res 30(5): 1393–1405
Graeff T, Zehe E, Schlaeger S, Morgner M, Bauer A, Becker R, Creutzfeldt B, Bronstert A (2010) A quality assessment of Spatial TDR soil moisture measurements in homogenous and heterogeneous media with laboratory experiments. Hydrol Earth Syst Sci 14:1007–1020
Grayson R, Blöschl G (eds) (2001) Spatial patterns in catchment hydrology observations and modelling. Cambridge University Press, Cambridge
Greco R (2006) Soil water content inverse profiling from single TDR waveforms. J Hydrol 317:325–339
Grote K, Hubbard S, Rubin Y (2002) Field-scale estimation of volumetric water content using GPR groundwave techniques. Wat Resour Res 39(11):1321. doi:10.1029/2003WR002045
Gurtz J, Zappa M, Jasper K, Lang H, Verbunt M, Badoux A, Vitvar T (2003) A comparative study in modelling runoff and its components in two mountainous catchments. Hydrol Process 17:297–311
Hajnsek I, Pottier E, Cloude SR (2003) Inversion of surface parameters from polarimetric SAR. IEEE Trans Geosci Remote Sens 41(4):727–744
Hajnsek I, Jagdhuber T, Schön H, Papathanassiou KP (2009) Potential of estimating soil moisture under vegetation cover by means of PolSAR. IEEE Trans Geosci Remote Sens 47(2):442–454
Harter T, Zhang D (1999) Water flow and solute spreading in heterogeneous soils with spatially variable water content. Wat Resour Res 35(2):415–426
Herkelrath WN, Hamburg SP, Murphy F (1991) Automatic real-time monitoring of soil moisture in a remote field area with time domain reflectometry. Wat Resour Res 27(5):857–864
Huisman JA, Sperl C, Bouten W, Verstraten JM (2001) Soil water content measurements at different scales: accuracy of time domain reflectometry and ground-penetrating radar. J Hydrol 245(1):48–58

Huisman JA, Snepvangers JJJC, Bouten W, Heuvelink GBM (2002) Mapping spatial variation in surface soil water content: comparison of ground-penetrating radar and time domain reflectometry. J Hydrol 269(3–4):194–207
Huisman JA, Hubbard S, Redman JD, Annan AP (2003) Measuring soil water content with ground penetrating radar: a review. Vadose Zone J 16:476–491
Jacobs JM, Meyers DA, Whitfield BM (2003) Improved rainfall/runoff estimates using remotely-sensed soil moisture. J Am Water Resour Ass 39(2):313–324
Jagdhuber T, Schön H, Hajnsek I, Papathanassiou KP (2009) Soil moisture estimation under vegetation applying polarimetric decomposition techniques. Proceedings of the 4th international workshop on science and applications of SAR polarimetry and polarimetric interferometry, Frascati, Italy, pp 1–8
Klok EJ, Jasper K, Roelofsma KP, Gurtz J, Badoux A (2001) Distributed hydrological modelling of a heavily glaciated Alpine river basin. Hydrol Sci J 46(4):553–570
Koyama C, Korres W, Fiener P, Schneider K (2010) Variability of surface soil moisture observed from multitemporal C-band synthetic aperture radar and field data. Vadose Zone J 9(4):1014–1024
Lakshmi V (2004) The role of satellite remote sensing in the prediction of ungauged basins. Hydrol Process 18(5):1029–1034
Lee J-S, Pottier E (2009) Polarimetric radar imaging from basics to applications. Taylor & Francis, Boca Raton
Lesmes DP, Friedman SP (2005) Relationships between the electrical and hydrogeological properties of rocks and soils, chap. 4. In: Rubin Y, Hubbard SS (eds) Hydrogeophysics. Springer, Dordrecht, pp 87–128
Marchi L, Borga M, Preciso E, Gaume E (2010) Characterisation of selected extreme flash floods in Europe and implications for flood risk management. J Hydrol 394(1–2):118–133
Martinez C, Hancock GR, Kalma J, Wells Z (2008) Spatio-temporal distribution of near-surface and root zone soil moisture at the catchment scale. Hydrol Process 22:2699–2714
Merz B, Bárdossy A (1998) Effects of spatial variability on the rainfall runoff process in a small loess catchment. J Hydrol 213(1–4):304–317
Merz B, Plate E (1997) An analysis of the effects of spatial variability of soil and soil moisture on runoff. Water Resour Res 33(12):2909–2922
Noto LV, Ivanov VY, Bras RL, Vivoni ER (2008) Effects of initialization on response of a fully-distributed hydrologic model. J Hydrol 352(1–2):107–125
Oswald B, Benedickter HR, Bächtold W, Flühler H (2003) Spatially resolved water content profiles from inverted time domain reflectometry signals. Wat Resour Res 39(12):1357
Parajka J, Naemi V, Blöschl G, Wagner W, Merz R, Scipal K (2006) Assimilating scatterometer soil moisture data into conceptual hydrologic models at coarse scales. Hydrol Earth Syst Sci 10:353–368
Pauwels RN, Hoeben R, Verhoest NEC, De Troch FP, Troch PA (2002) Improvements of TOPLATS-based discharge predictions through assimilation of ERS-based remotely-sensed soil moisture values. Hydrol Proc 16:995–1013
Pilgrim DH, Cordery I (1993) Flood runoff. In: Maidment DR (ed) Handbook of hydrology. McGraw-Hill, Inc., New York
Refsgaard JC (1997) Validation and intercomparison of different updating procedures for real-time forecasting. Nordic Hydrol 28:65–84
Robinson DA, Jones SB, Wraith JM, Or D, Friedman SP (2003) A review of advances in dielectric and electrical conductivity measurement in soils. Vadose Zone J 2:444–475
Robinson DA, Abdu H, Jones SB, Seyfried M, Lebron I, Knight R (2008a) Soil moisture measurement for ecological and hydrological watershed-scale observatories: a review. Vadose Zone J 7:358–389
Robinson DA, Campbell JW, Hopmans BK, Hornbuckle SB, Jones R, Knight R, Odgen R, Selker J, Wendroth O (2008b) Eco-geophysical imaging of watershed-scale soil patterns links with plant community spatial patterns. Vadose Zone J 7:1132–1138
Ryu D, Famiglietti JS (2005) Characterization of footprint-scale surface soil moisture variability using Gaussian and beta distribution functions during the Southern Great Plains 1997 (SGP97) hydrology experiment. Water Resour Res 41(12), W12433. doi:10.1029/2004WR003835
Schlaeger S (2005) A fast TDR-inversion technique for the reconstruction of spatial soil moisture content. Hydrol Earth Syst Sci 9:481–492
Schmalholz J (2007) Georadar for small-scall high-resolution dielectric property and water content determination of soils. Technische Universität, Berlin
Schulla J (1997) Hydrologische Modellierung von Flussgebieten zur Abschätzung der Folgen von Klimaänderungen. Züricher Geographische Schriften, ETH Zürich
Schulla J, Jasper K (2007) Model description WaSiM-ETH. Technical report, Zürich

Taumer K, Stoffregen H, Wessolek G (2006) Seasonal dynamics of preferential flow in a water repellent soil. Vadose Zone J 5(1):405–411

Uhlenbrook S, Leibundgut C (2002) Process-oriented catchment modeling and multiple-response validation. Hydrol Proc 16:423–440

Van Overmeeren RA, Sariowan SV, Gehrels JC (1997) Ground penetrating radar for determining volumetric soil water content: results of comparative measurements at two test sites. J Hydrol 197:316–338

van Zyl JJ, Arii M, Ki Y (2008) Requirements for model-based polarimetric decompositions. Proceedings of the 7th European conference on synthetic aperture radar (EUSAR), Friedrichshafen, Germany, pp 41–44

Vereecken H, Kamai T, Harter T, Kasteel R, Hopmans J, Vanderborght J (2007) Explaining soil moisture variability as a function of mean soil moisture: a stochastic unsaturated flow perspective. Geophys Res Lett 34:L22402. doi:10.1029/2007GL031813

Vereecken H, Huisman JA, Bogena H, Vanderborght J, Vrugt JA, Hopmans JW (2008) On the value of soil moisture measurements in vadose zone hydrology: a review. Wat Resour Res 44:W00D06. doi:10.1029/2008WR006829

Wagner W, Blöschel G, Pampaloni P, Calvet J-C, Bizarri B, Wigneron J-P, Kerr Y (2004) Operational readiness of microwave remote sensing of soil moisture for hydrologic applications. Nordic Hydrol 38(1):1–20

Weihermuller L, Huisman JA, Lambot S, Herbst M, Vereecken H (2007) Mapping the spatial variation of soil water content at the field scale with different ground penetrating radar techniques. J Hydrol 340(3–4):205–216

Weiler M, McDonnell JJ (2007) Conceptualizing lateral preferential flow and flow networks and simulating the effects on gauged and ungauged hillslopes. Water Resour Res 43:W03403

Weissling BP, Xie H, Murray KE (2007) A multitemporal remote sensing approach to parsimonious streamflow modeling in a southcentral Texas watershed, USA. Hydrol Earth Syst Sci 4:1–33

Western A, Grayson R, Blöschl G (2002) Scaling of soil moisture: a hydrologic perspective. Ann Rev Earth Planet Sci 30:149–180

Wollny K (1999) Die Natur der Bodenwelle des Georadar und ihr Einsatz zur Feuchtebestimmung. Utz, Wiss., München

Yamaguchi Y, Moriyama T, Ishido M, Yamada H (2005) Four-component scattering model for polarimetric SAR image decomposition. IEEE Trans Geosci Remote Sens 43(8):1699–1706

Younis J, Anquetin S, Thielen J (2008) The benefit of high-resolution operational weather forecasts for flash flood warning. Hydrol Earth Syst Sci 12(4):1039–1051

Zehe, E., Blöschl, G. (2004) Predictability of hydrologic response at the plot and catchment scales—the role of initial conditions. Water Resour Res 40(10):W10202. doi:10.1029/2003WR002869

Zehe E, Becker R, Bárdossy A, Plate E (2005) Uncertainty of simulated catchment sale runoff response in the presence of threshold processes: role of initial soil moisture and precipitation. J Hydrol 315(1–4):183–202